

Supporting Information

Reduction of Imines with a Reusable Bimetallic PdCo–Fe₃O₄ Catalyst at Room Temperature under Atmospheric Pressure of H₂

Sabyuk Yang and Byeong Moon Kim*

Department of Chemistry, College of Natural Sciences, Seoul National University, Seoul
08826, South Korea.

Table of Contents

I. Experimental section

1. General information.....	S3
2. Experimental procedures of the synthesis of catalysts.....	S8
3. Supplementary reaction optimization data	
· Table S1. Solvent screening.....	S11
· Table S2. Catalyst screening.....	S12
· Table S3. Catalyst loading screening.....	S13
· Table S4. Reductant screening.....	S14
4. Characterization of catalysts	
· Figure S1. SEM analysis.....	S15
· Figure S2. SEM-EDS analysis.....	S16
· Figure S3. EDS map spectrum.....	S19
· Figure S4. HR-TEM analysis.....	S20
· Figure S5. BF-STEM and HADDF-STEM analysis.....	S22
· Figure S6. Particle distribution of PdCo–NPs.....	S24
· Figure S7. EELS spectrum.....	S26
· Figure S8. XRD analysis.....	S27
· Figure S9. XPS data.....	S28
· Figure S10. FTIR analysis.....	S30
· Figure S11. ICP-AES analysis.....	S31

5. Supplementary data	
· Figure S12. SEM, EDS, and ICP-AES analysis of $\text{Pd}_x\text{Co}_y\text{--Fe}_3\text{O}_4$	S32
· Figure S13. Recycling data of various $\text{Pd}_x\text{Co}_y\text{--Fe}_3\text{O}_4$	S37
· Figure S14. SEM analysis of recycled catalyst.....	S38
· Figure S15. HR-TEM analysis of recycled catalyst.....	S39
· Figure S16. SEM analysis of other PdCo–NPs.....	S40
· Table S5. ICP-AES of other PdCo–NPs.....	S40
· Table S6. Yield comparison of monometallic catalysts with other substrates.....	S41
· Figure S17. Kinetic data of imine reduction.....	S42
6. Characterization of products.....	S43
II. References.....	S49
III. NMR spectra.....	S50

I. Experimental section

1. General information

All 1D NMR spectroscopy experiments were conducted with a DD2MR400 (400 MHz, Agilent Technologies, Santa Clara, CA, USA) or Varian 500 (500 MHz, Varian, Inc., Palo Alto, CA, USA). NMR spectra were processed with MestReNova. Chemical shifts are reported in ppm and referenced to residual solvent peaks (CHCl_3 in CDCl_3 : 7.26 ppm for ^1H , 77 ppm for ^{13}C). Coupling constants are reported in Hertz. All commercially available chemicals were purchased from Acros Organics (Pittsburgh, PA, USA), Sigma-Aldrich Aldrich (St. Louis, MO, USA), Alfa Aesar (Ward Hill, MA, USA), or Tokyo Chemical Industry (Tokyo, Japan), and used without further purification. Imine substrates were synthesized by a known procedure.^[1]

Catalyst characterization

SEM images were obtained using JSM-7800F Prime (JEOL Ltd., Tokyo, Japan) and MERLIN Compact (ZEISS, Oberkochen, Germany). HR-TEM images were obtained using JEM-3010 (JEOL Ltd., Tokyo, Japan). STEM images were obtained using JEM-ARM200F (JEOL Ltd., Tokyo, Japan). XPS data were obtained using SIGMA PROBE (ThermoVG, U.K.). ICP-AES data were obtained using OPTIMA 8300 (Perkin-Elmer, Waltham, MA, USA). The machines mentioned above are installed at the National Center for Inter-University Research Facilities (NCIRF) at Seoul National University. EELS images were obtained using Themis Z (Thermo Fisher, MA, USA) installed at the Research Institute of Advanced Materials (RIAM) at Seoul National University.

The powder X-ray diffraction (XRD) was performed using a D8 Advance (Bruker, Billerica, MA, USA) installed at the National Instrumentation Center for Environmental Management (NICEM) at Seoul National University.

Fourier-transform infrared spectroscopy images were obtained using Spectrum Two (Perkin-Elmer, Waltham, MA, USA) installed at Seoul National University.

General Procedure of the Synthesis of Amines

A glass vial (10 mL) were charged with an imine (0.20 mmol), PdCo–Fe₃O₄ (2.0 mol%), and *N,N*-dimethylacetamide (1.0 mL). The mixture was sonicated for 1 min and stirred at room temperature. Next, the vial was purged with H₂ using a balloon filled with H₂ for 1 min and stirred for 18 h at room temperature. The reaction mixture was extracted by ethyl acetate and the organic layer was filtered through a layer of Celite^R and magnesium sulfate. The crude product was purified by column chromatography.

Materials/Instrumentation

ESCA (Electron Spectroscopy for Chemical Analysis)

1. Model: SIGMA PROBE (ThermoVG, U.K)
2. Electron analyzer with Lens system
 - 2.1 Type: Spherical sector analyzer, 180 degree
 - 2.2 Mean diameter: 275 mm or equivalent
 - 2.3 Analysis area: 15 um to 400 um,
 - 2.4 Detector: Multi channeltron detectors
3. UHV Analysis chamber
 - 3.1 Material: 100% mu- metal chamber or equivalent
 - 3.2 Ultimate vacuum: 5 x 10⁻¹⁰ mbar or better (Ti-sub pump)
4. Monochromator X-ray source
 - 4.1 Type: Microfocused monochromator source
 - 4.2 Electron gun: 15 kv or better
 - 4.3 Anode: Moveable Al

5. SEM/SAM/AES

- 5.1 Type: with field Schottky Field emission source
- 5.2 Beam Energy: 1 keV - 10 keV
- 5.3 SEM resolution: < 95 nm*, at 10 keV, 5.0 nA
- 5.4 Beam Current: Up to 50 nA
- 5.5 SAM resolution: < 250 nm*, at 3 keV, 5.0 nA

6. Ion source

- 6.1 Energy range: 0.1 keV to 4 keV, continuously variable
- 6.2 Max. beam current density: 3 mA/cm² or equivalent
- 6.3 Min. Beam diameter: 200 um or equivalent

7. Electron flood gun for charge compensation

Transmission Electron Microscope II (ccd camera type)

- 1. Model: JEM-3010 (JEOL Ltd., Tokyo, Japan)
- 2. Accelerating Voltage: 80 to 300 Kv
- 3. Gatan Digital Camera (MSC-794)
- 4. Resolution: Point image: 0.17 nm
Lattice image: 0.14 nm
- 5. MAG: x50 ~ x1,500,000
- 6. Camera Length: SA DIFF Mode: 120 ~ 3,000 mm

Cs-STEM (Cs corrected STEM with Cold FEG)

- 1. Model: JEM-ARM200F (JEOL Ltd., Tokyo, Japan)
- 2. Specifications
 - a. HT: 60, 80, 120, 200 kV

- b. Magnification: 50 to 2,000,000 X (TEM), 200 to 1,500,000 X (STEM)
 - c. Resolution
 - STEM mode: HAADF 0.08 nm/ BF 0.136 nm
 - TEM mode: Point 0.23 nm
 - d. Sample tilting
 - X / Y: $\pm 35^\circ$ / $\pm 30^\circ$
3. Analysis functions
- a. CCD Camera: OneView camera (25 fps at full 4k x 4k resolution)
 - b. EDS: SDD Type (Active area 100mm²/ Solid angle 0.9 sr)
 - c. EELS: Model 965 GIF Quantum ER

EELS (Cs corrected monochromated TEM/STEM)

- 1. Accelerating voltage: 60-300 kV (60, 80, 200, 300)
- 2. Resolution
 - Image corrector: Information Limit 70 pm, STEM resolution 136 pm
 - Probe corrector: Information Limit 100 pm, STEM resolution 60 pm
 - X-FEG/ monochromator + image corrector: Information Limit 60 pm, STEM resolution 60 pm
- 3. EDS energy resolution at Mn \leq 136 eV (all detectors): 133.4 eV
- 4. Monochromator energy resolution: 300 kV: 0.17 eV, 200 kV: 0.14 eV, 80 kV: 0.17 eV, 60 kV: 0.16 eV
- 5. HR-STEM resolution (HAADF with S-CORR \leq 0.06 nm): 0.05 nm

Fourier-transform infrared spectroscopy

Wavenumber Range: 8300 ~ 350 cm⁻¹ optimized, proprietary KBr beam splitter

Interferometer: Rotary Michelson interferometer

Signal to Noise: 9,300:1 peak-peak, 5 seconds

Wavenumber accuracy: Better than 0.01 cm⁻¹ at 3,000 cm⁻¹

Resolution: 0.5 cm⁻¹ standard

IQ/OQ support

Size: 450 mm x 300 mm x 210 mm (W x D x H)

Communication: USB, wireless and TCP/IP

AVI (Absolute Virtual Instrument) option

Weight: 13 kg

2. Experimental procedures of the synthesis of catalysts

Synthesis of PdCo–Fe₃O₄ NPs

Initially, 88.7 mg (0.50 mmol) of PdCl₂ and 1.00 g of PVP (Mw~10,000 g mol⁻¹, 0.10 mmol) were placed in 20 mL of ethylene glycol (EG) in a 100 mL round-bottom flask. This mixture was sonicated for 10 min and stirred for 1 h at 100 °C in an oil bath. In a separate 100 mL round-bottom flask, 119.0 mg (0.50 mmol) of CoCl₂·6H₂O and 500 mg of PVP (0.050 mmol) were added to 20 mL of water. This mixture was sonicated for 10 min and stirred for 30 min at 60 °C in an oil bath. Meanwhile, 500 mg of Fe₃O₄ NPs were added to 150 mL of water in a two-necked 500 mL round-bottom flask and then sonicated for 10 min. The prepared Pd precursor solution was then injected dropwise onto the Fe₃O₄ suspension with vigorous stirring. After 5 min, the Co precursor solution was added and 90 mg (2.38 mmol) of sodium borohydride in 20 mL of water was injected dropwise. The resulting mixture was stirred for 24 h at 60 °C. Subsequently, the PdCo alloy on Fe₃O₄ nanoparticles was retrieved via sonication and washing with ethanol (40 mL x 10 times) and dried on a rotary evaporator to give PdCo–Fe₃O₄ NPs (550 mg, 77% yield based on PdCl₂).

Synthesis of Pd–Fe₃O₄ NPs

Initially, 177 mg of PdCl₂ (1.0 mmol) and 2.00 g of PVP (0.20 mmol) were placed in 40 mL of EG in a 100 mL round-bottom flask. This mixture was sonicated for 10 min and stirred for 1 h at 100 °C. Meanwhile, 500 mg of Fe₃O₄ NPs was added to 150 mL of EG in a two-necked 500 mL round-bottom flask. The prepared precursor solution was then injected dropwise to Fe₃O₄ NPs in 150 mL of EG, and stirred at 100 °C for an additional 24 h. The resultant product was washed with ethanol (40 mL x 10 times) and dried on a rotary evaporator to give Pd–Fe₃O₄ NPs (440.0 mg, 36% yield based on PdCl₂).

Synthesis of Co–Fe₃O₄ NPs

Initially, 23.8 mg of CoCl₂·6H₂O (0.30 mmol) and 200 mg of PVP (0.020 mmol) were placed in 4.0 mL of water in a 10 mL round-bottom flask. This solution was sonicated for 1 min and stirred for 30 min at 60 °C. Meanwhile, 100 mg of Fe₃O₄ NPs was added to 30 mL of water in a two-necked 100 mL round-bottom flask. The prepared precursor solution was then injected dropwise to Fe₃O₄ NPs in 30 mL of water, followed by dropwise addition of 30 mg of sodium borohydride (0.79 mmol) in 4.0 mL of water. The mixture was stirred at 60 °C for an additional 24 h. The resultant product was washed with ethanol (40 mL x 10 times) and dried on a rotary evaporator to give Co–Fe₃O₄ NPs (98.5 mg, 30% yield based on CoCl₂·6H₂O).

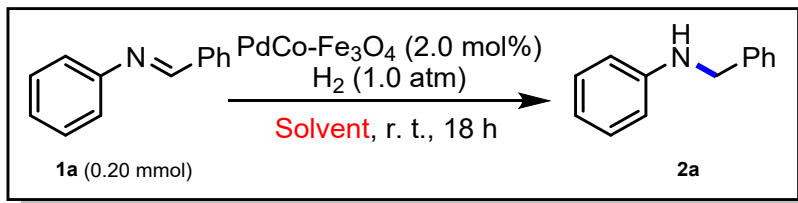
Synthesis of Pd_xCo_y–Fe₃O₄ NPs

For Pd_xCo_y–Fe₃O₄ synthesis, the same method used for the synthesis of PdCo–Fe₃O₄ NPs was employed, with different quantities of metals. To prepare Pd_{0.26}Co₁–Fe₃O₄ NPs, PdCl₂ (6.6 mg, 0.038 mmol) with PVP (0.0060 mmol), CoCl₂·6H₂O (35.7 mg, 0.15 mmol) with PVP (0.010 mmol), and sodium borohydride (0.79 mmol) were used. For the synthesis of Pd_{0.46}Co₁–Fe₃O₄ NPs, PdCl₂ (11.1 g, 0.063 mmol) with PVP (0.010 mmol), CoCl₂·6H₂O (35.7 mg, 0.15 mmol) together with PVP (0.010 mmol), and sodium borohydride (0.79 mmol) were used. In the case of Pd₁Pd_{0.45}–Fe₃O₄ NPs, PdCl₂ (17.7 mg, 0.10 mmol) with PVP (0.020 mmol), CoCl₂·6H₂O (18.2 mg, 0.077 mmol) with PVP (0.0050 mmol), and sodium borohydride (0.79 mmol) were used. Finally, for the preparation of Pd₁Co_{0.28}–Fe₃O₄ NPs, PdCl₂ (17.7 mg, 0.10 mmol) with PVP (0.020 mmol), CoCl₂·6H₂O (11.1 mg, 0.047 mmol) with PVP (0.0030 mmol), and sodium borohydride (0.79 mmol) were used. Meanwhile, 100 mg of Fe₃O₄ NPs were added to 30 mL of water in a two-necked 100 mL round-bottom flask and then sonicated for 10 min. The prepared Pd precursor solution in 4.0 mL of EG was then injected dropwise onto the Fe₃O₄ suspension with vigorous stirring. After 5 min, the Co precursor solution in 4.0 mL of water was added and sodium borohydride in 4.0 mL of water was injected dropwise. The resulting mixture was stirred for 24 h at 60 °C. Subsequently, the Pd_xCo_y alloy on Fe₃O₄

nanoparticles was retrieved via sonication and washing with ethanol (40 mL x 10 times) and dried on a rotary evaporator to give $\text{Pd}_{0.26}\text{Co}_1\text{--Fe}_3\text{O}_4$ NPs (99.0 mg, 59% yield based on PdCl_2), $\text{Pd}_{0.46}\text{Co}_1\text{--Fe}_3\text{O}_4$ NPs (96.0 mg, 57% yield based on PdCl_2), $\text{Pd}_1\text{Co}_{0.45}\text{--Fe}_3\text{O}_4$ NPs (98.0 mg, 42% yield based on $\text{CoCl}_2 \cdot 6\text{H}_2\text{O}$), and $\text{Pd}_1\text{Co}_{0.28}\text{--Fe}_3\text{O}_4$ NPs (98.0 mg, 69% yield based on $\text{CoCl}_2 \cdot 6\text{H}_2\text{O}$).

3. Supplementary reaction optimization data

Table S1. Solvent screening^a

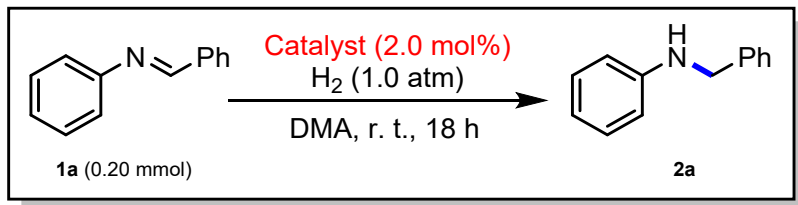


Entry	Solvent	Conversion (%) ^b	1a (%) ^b	Aniline (%) ^b	Yield (%) ^b
1	MeOH	99	1	16	71
2	EtOH	99	1	13	75
3	<i>t</i> BuOH	99	1	0	77
4	H_2O	97	3	10	85
5	THF	99	1	0	72
6	DMF	99	1	0	83
7	DMA	99	1	0	95
8	Acetone	99	1	0	84
9	HFIP	100	0	72	N. D. ^c
10	CH_3CN	99	1	0	74

^a Reaction conditions: **1a** (0.20 mmol), $\text{PdCo-Fe}_3\text{O}_4$ (2.0 mol%), H_2 (1.0 atm), solvent (1.0 mL), r. t., 18 h.

^b Determined from GC analysis through the use of mesitylene as an internal standard.

^c N. D. = not detected.

Table S2. Catalyst screening^a

Entry	Catalyst (mol%)	Conversion (%) ^b	1a (%) ^b	Aniline (%) ^b	Yield (%) ^b
1	Fe ₃ O ₄	0	100	0	N. D. ^c
2 ^d	Pd/C (4.0)	100	0	>99	N. D.
3	Pd–Fe ₃ O ₄ (4.0)	60	40	0	60
4	Co–Fe ₃ O ₄ (4.0)	0	100	0	N. D.
5	PdCo–Fe ₃ O ₄ (2.0)	99	1	0	95
6	Pd–Fe ₃ O ₄ (2.0) + Co–Fe ₃ O ₄ (2.0)	72	28	0	72

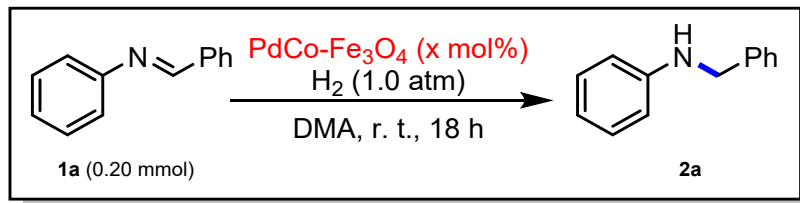
^a Reaction conditions: **1a** (0.20 mmol), catalyst (x mol%) H₂ (1.0 atm), DMA (1.0 mL), r. t., 18 h.

^b Determined from GC analysis through the use of mesitylene as an internal standard.

^c N. D. = not detected.

^d Byproducts generated from hydrogenolysis were detected.

Table S3. Catalyst loading screening^a



Entry	Catalyst loading (mol%)	TON ^c	Conversion (%) ^b	1a (%) ^b	Yield (%) ^b
1 ^d	0.01	550	21	79	11
2 ^e	0.03	1583	100	4	95
3 ^f	0.05	910	100	3	91
4 ^g	0.10	440	100	3	88
5	0.50	98	100	0	98
6	1.0	50	100	0	>99
7	1.5	30	100	0	91
8	2.0	24	99	1	95

^a Reaction conditions: **1a** (0.20 mmol), $\text{PdCo-Fe}_3\text{O}_4$ (x mol%), H_2 (1.0 atm), DMA (1.0 mL), r. t., 18 h.

^b Determined from GC analysis through the use of mesitylene as an internal standard.

^c Turnover number (TON)=mmol of product/mmol of total metal except Fe

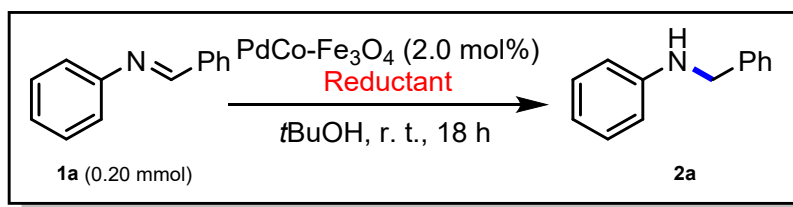
^d Result with **1a** (10 mmol), DMA (3.0 mL), 52 h.

^e Result with **1a** (3.3 mmol), DMA (1.0 mL), 78 h.

^f Result with **1a** (2.0 mmol), DMA (1.0 mL), 48 h.

^g Result with **1a** (1.0 mmol), DMA (1.0 mL), 48 h.

Table S4. Reductant screening^a



Entry	Reductant	Conversion (%) ^b	1a (%) ^b	Aniline (%) ^b	Yield (%) ^b
1	PhSiH ₃	90	10	12	54
2	BH ₃ NH ₃	69	31	7	56
3	NaBH ₄	23	77	6	17

^a Reaction conditions: **1a** (0.20 mmol), PdCo-Fe₃O₄ (x mol%), *t*BuOH (1.0 mL), reductant (3.0 equiv), r. t., 18 h.

^b Determined from GC analysis through the use of mesitylene as an internal standard.

4. Characterization of Catalysts

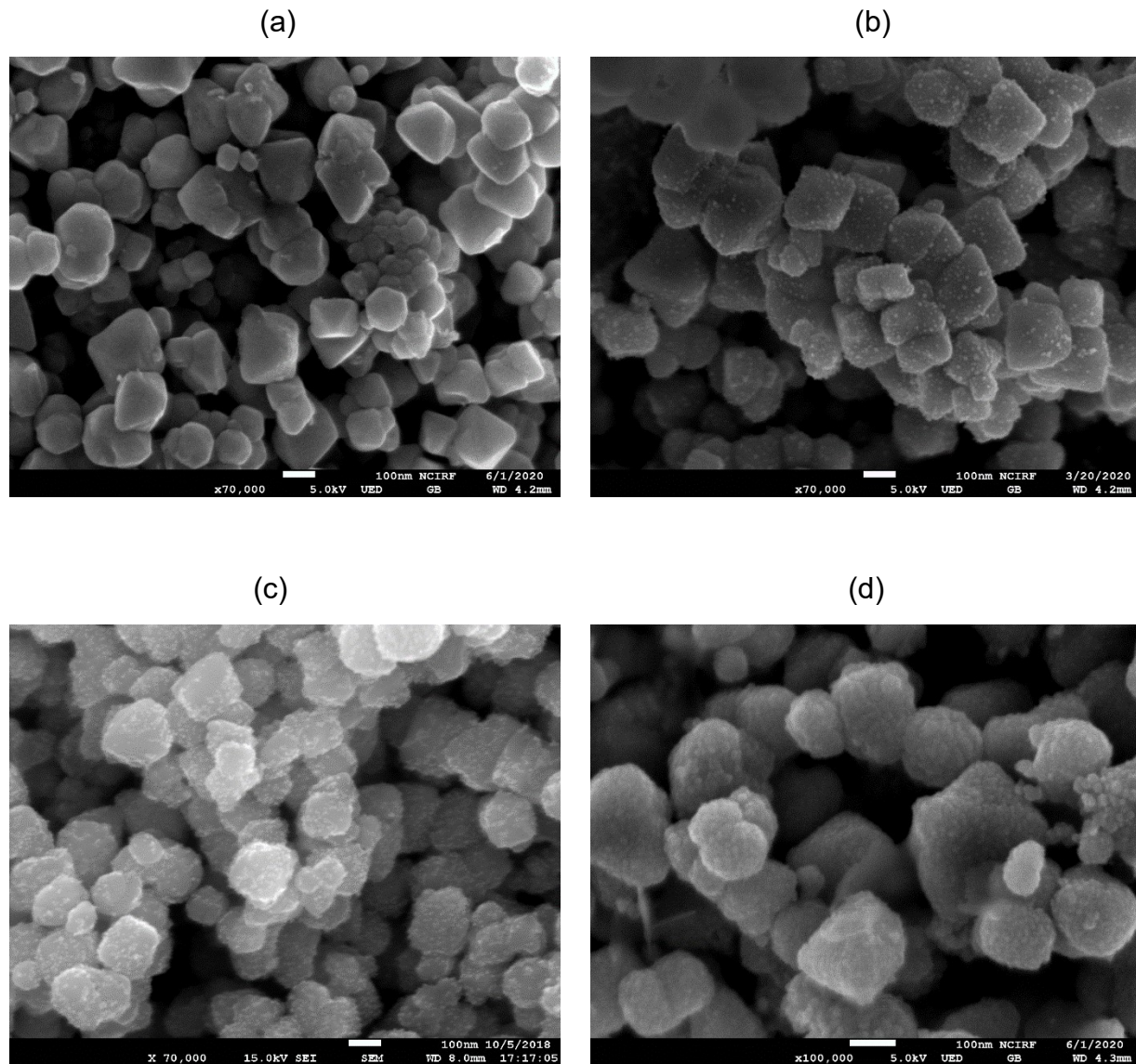
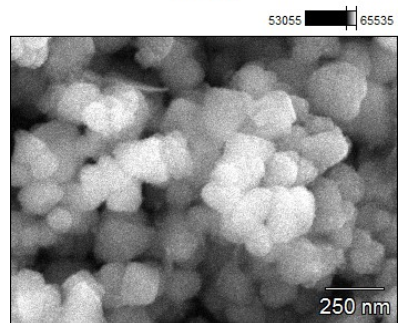


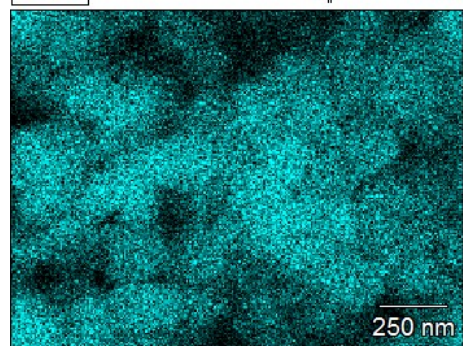
Figure S1. SEM image of (a) Fe_3O_4 NPs; (b) PdCo– Fe_3O_4 NPs; (c) Pd– Fe_3O_4 NPs; and (d) Co– Fe_3O_4 NPs

(a)

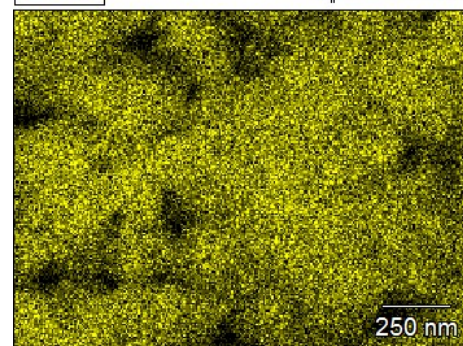
Base(1)



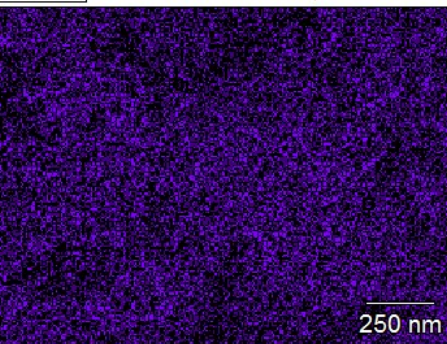
OK



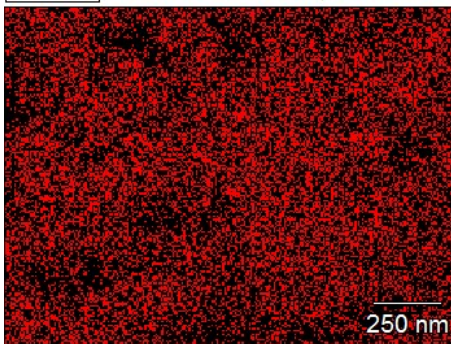
Fe K



Pd L

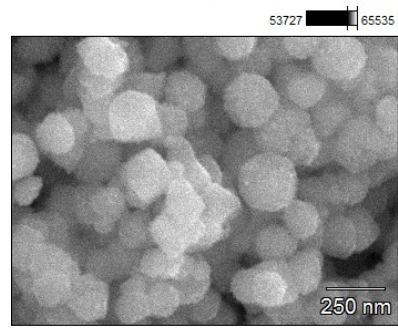


Co K



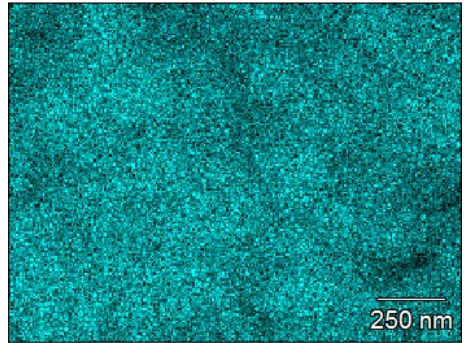
(b)

Base(3)



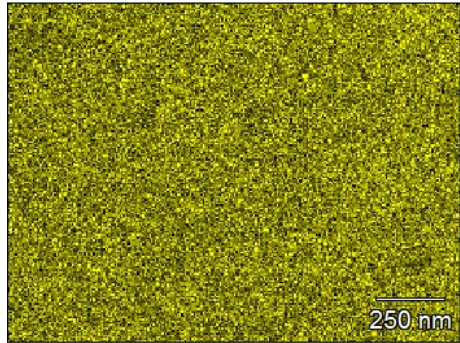
OK

0 20



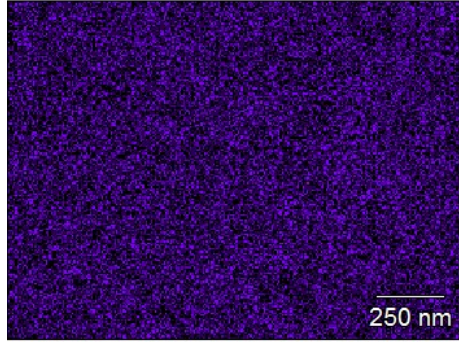
Fe K

0 15



Pd L

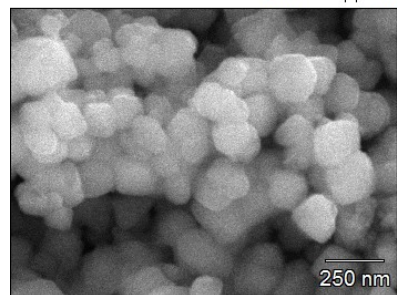
0 8



(c)

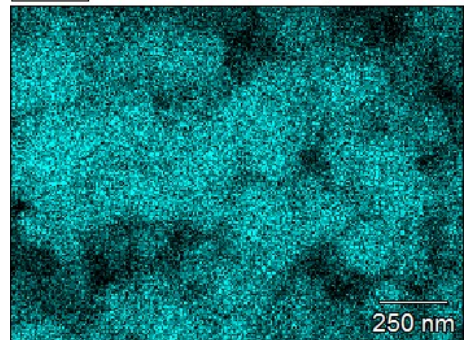
Base(5)

52871 65535



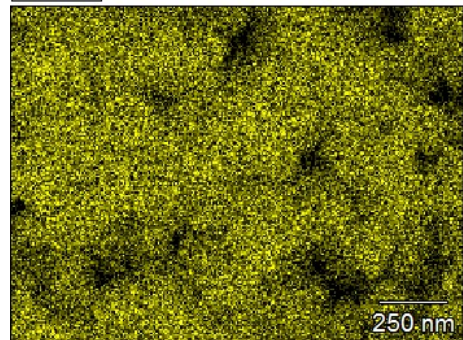
OK

0 16



Fe K

0 13



Co K

0 6

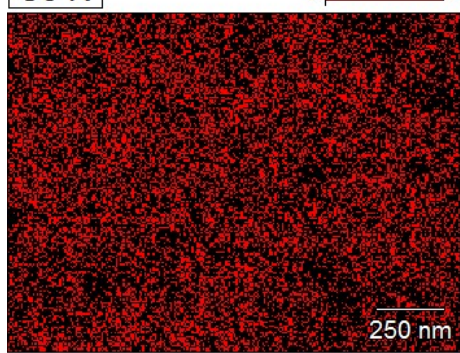


Figure S2. (a) SEM-EDS images of PdCo- Fe_3O_4 NPs; (b) SEM-EDS images of Pd- Fe_3O_4 NPs; and (c) SEM-EDS images of Co- Fe_3O_4 NPs

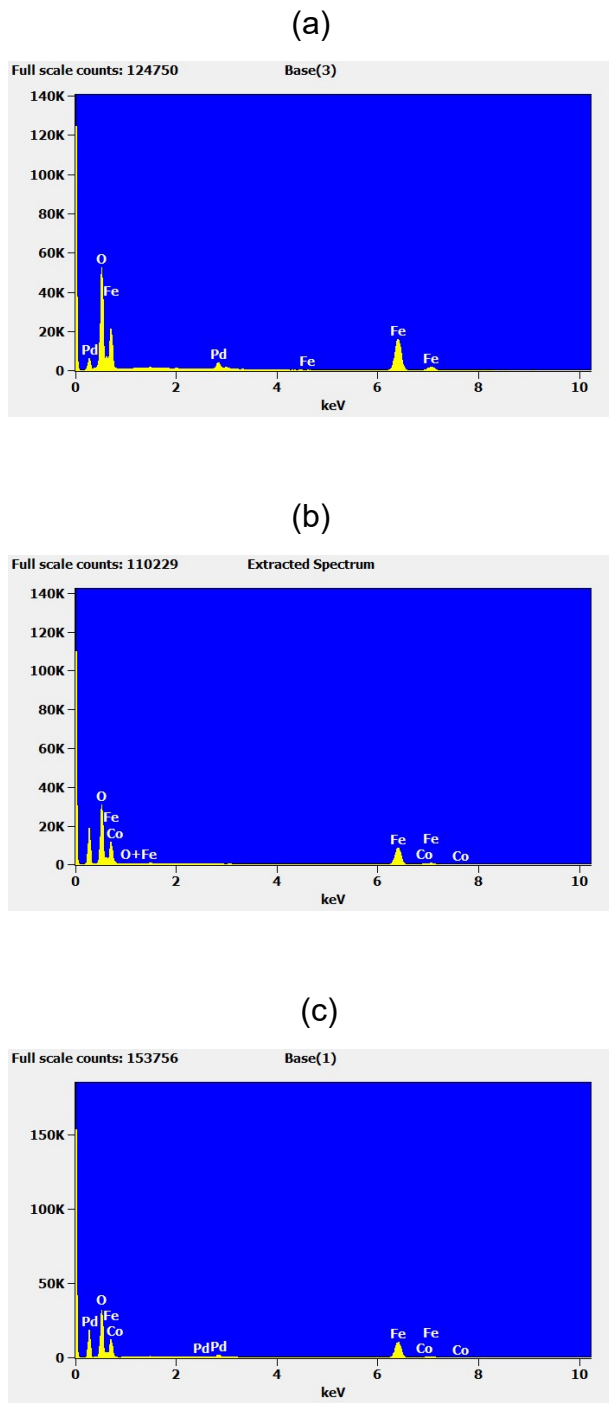
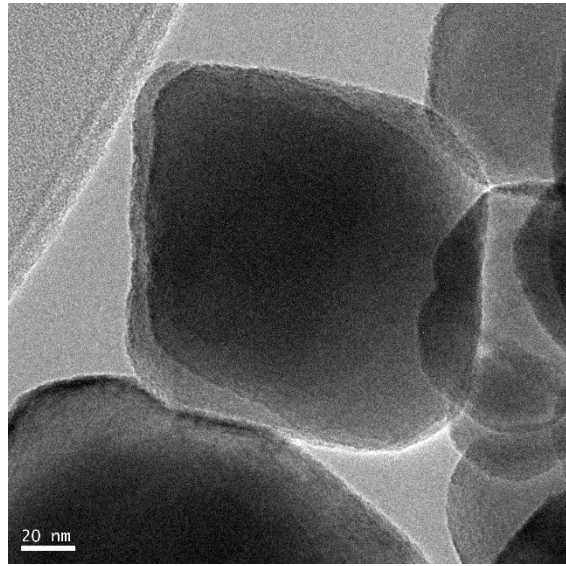
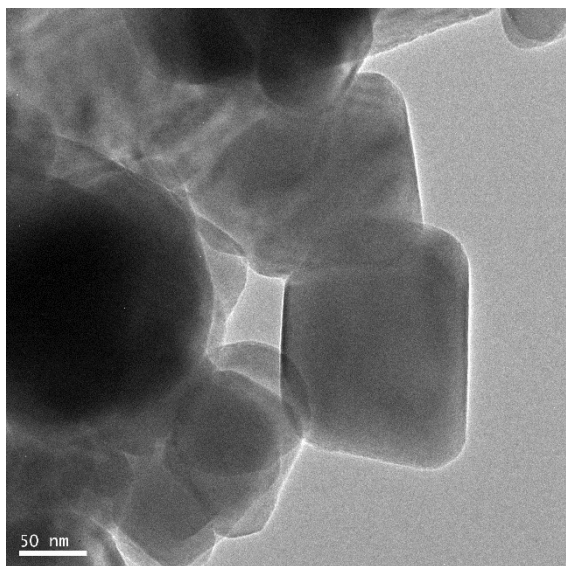


Figure S3. The energy disperse spectroscopy (EDS) map sum spectrum pattern of NPs; (a) Pd–Fe₃O₄ NPs; (b) Co–Fe₃O₄ NPs; and (c) PdCo–Fe₃O₄ NPs

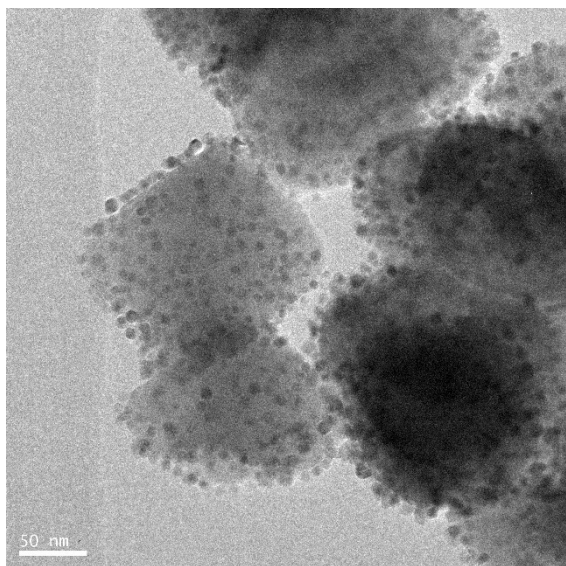
(a)

S19

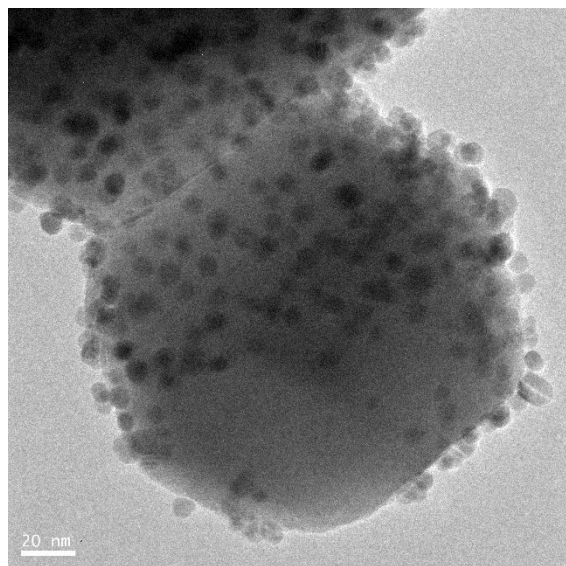
(b)



(c)



(d)



(e)

(f)

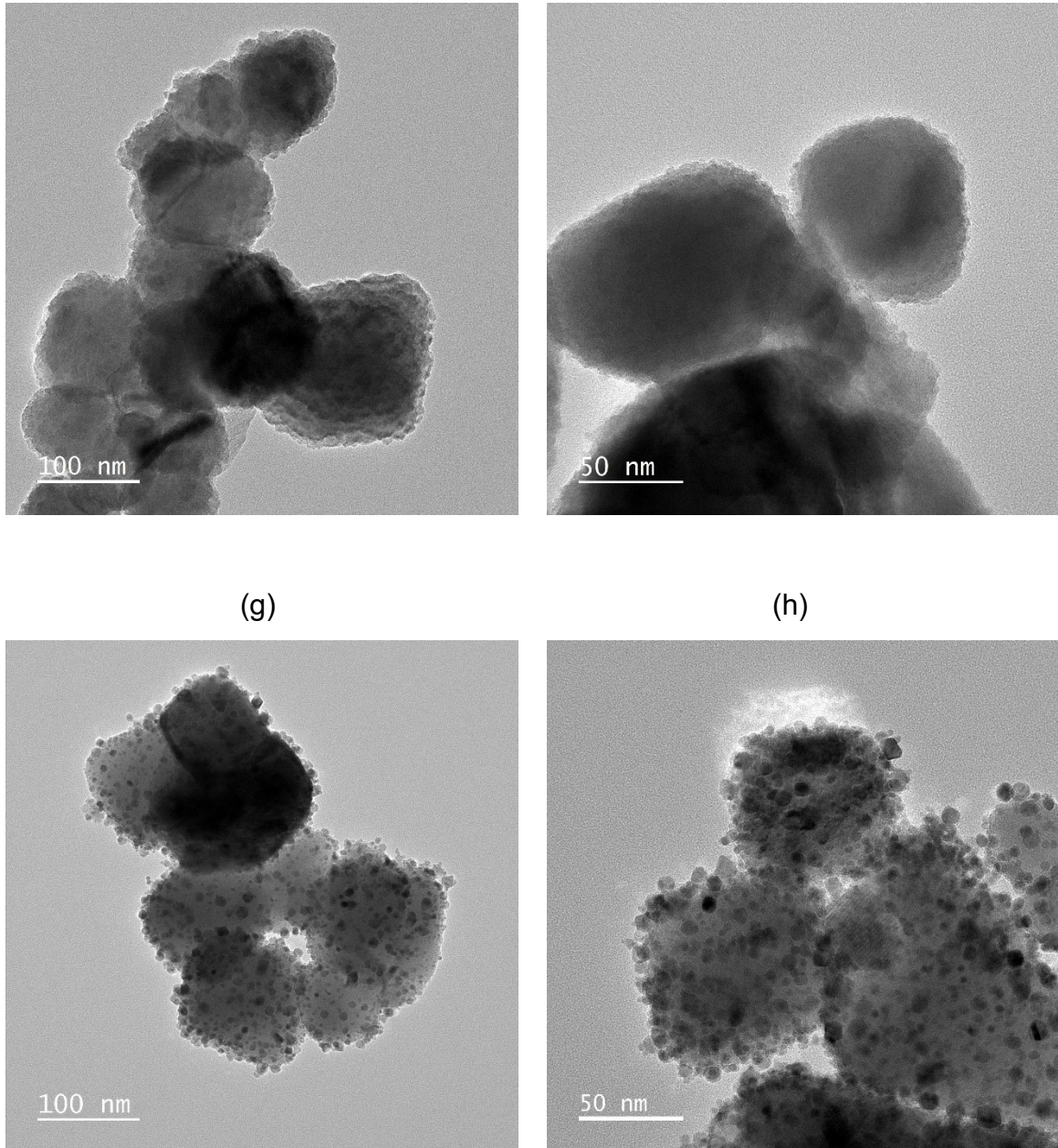
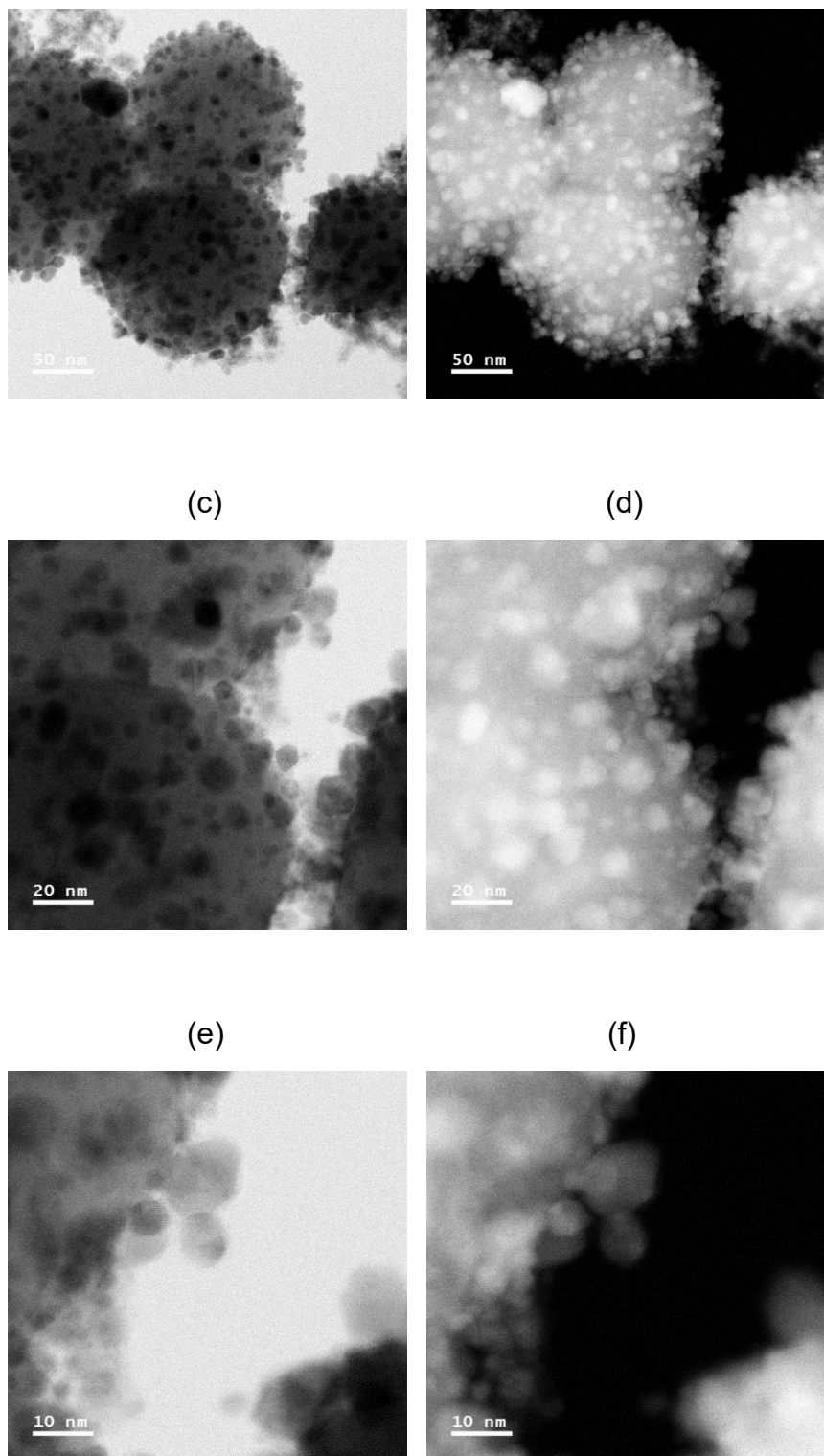


Figure S4. HR-TEM images of (a) and (b) Fe_3O_4 NPs; (c) and (d) $\text{Pd}-\text{Fe}_3\text{O}_4$ NPs; (e) and (f) $\text{Co}-\text{Fe}_3\text{O}_4$ NPs; (g) and (h) $\text{PdCo}-\text{Fe}_3\text{O}_4$ NPs

(a)

(b)



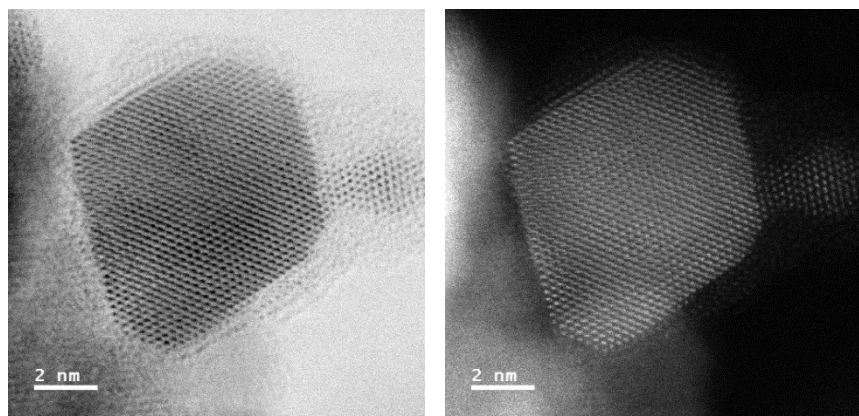
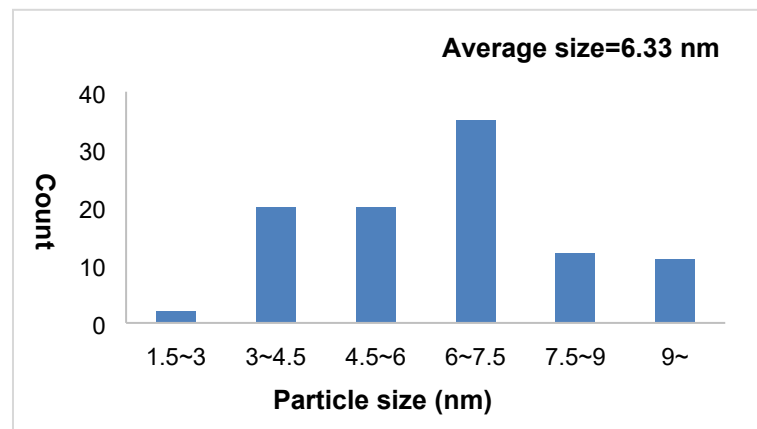
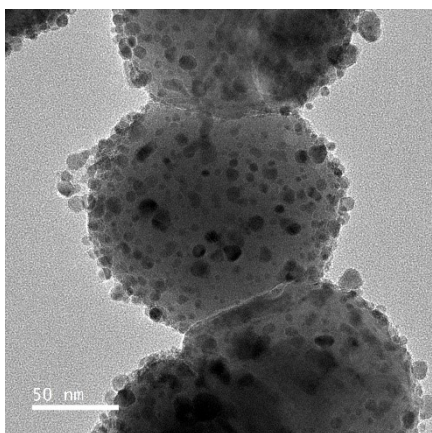
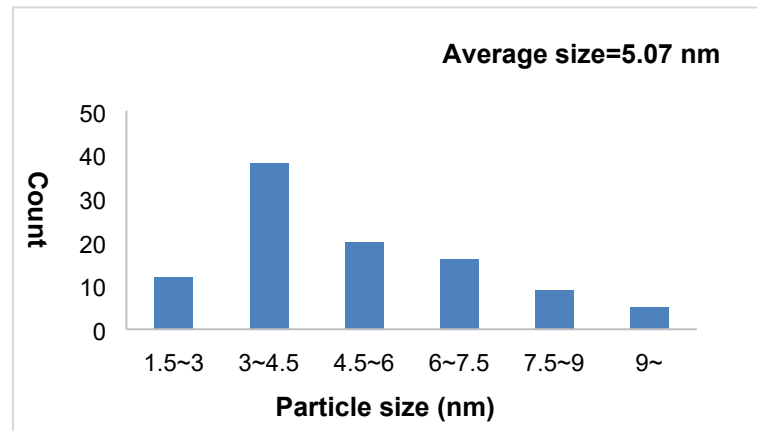
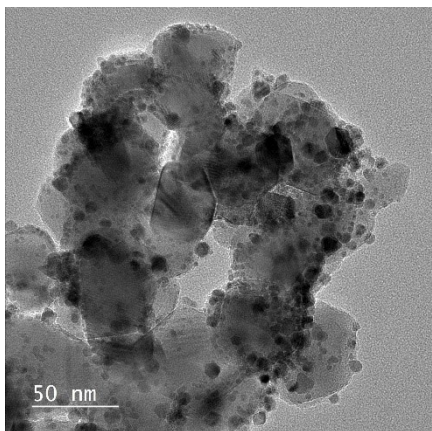


Figure S5. (a), (c), (e), and (g) BF-STEM images of PdCo–Fe₃O₄ NPs; (b), (d), (f), and (h) HADDF-STEM images of PdCo–Fe₃O₄ NPs

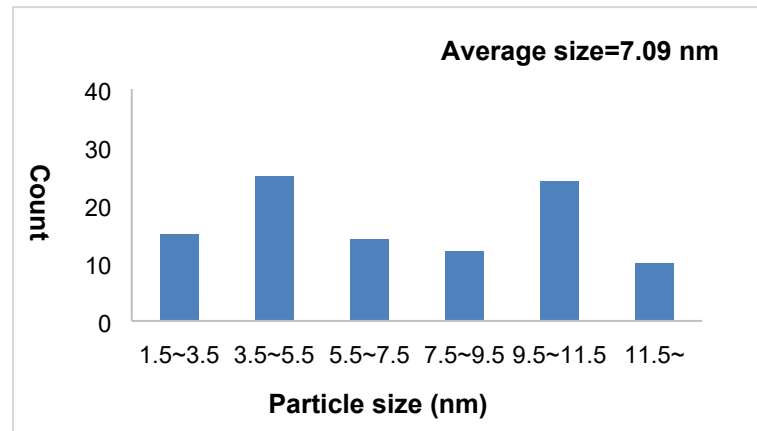
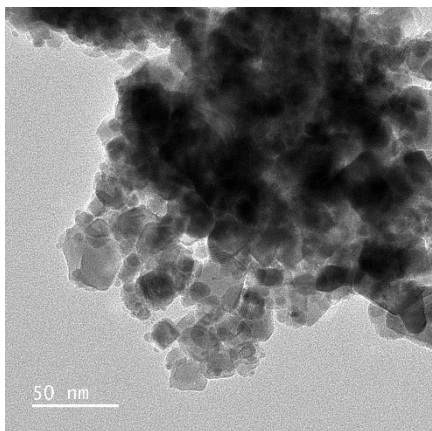
(a)



(b)



(c)



(d)

S24

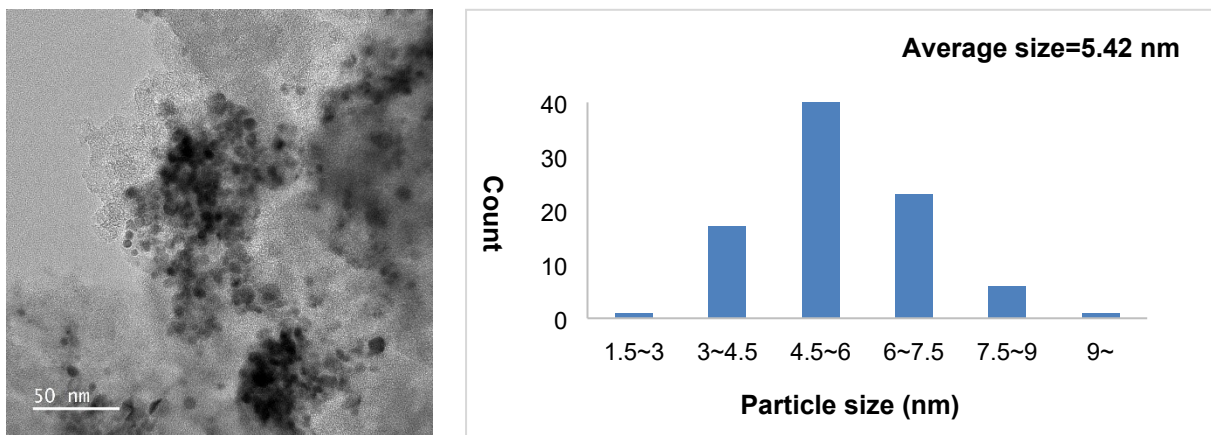


Figure S6. HR-TEM images and particle distribution of (a) PdCo–Fe₃O₄ NPs; (b) PdCo–TiO₂ NPs; (c) PdCo–CeO₂ NPs; and (d) PdCo–C NPs

(a)

(b)

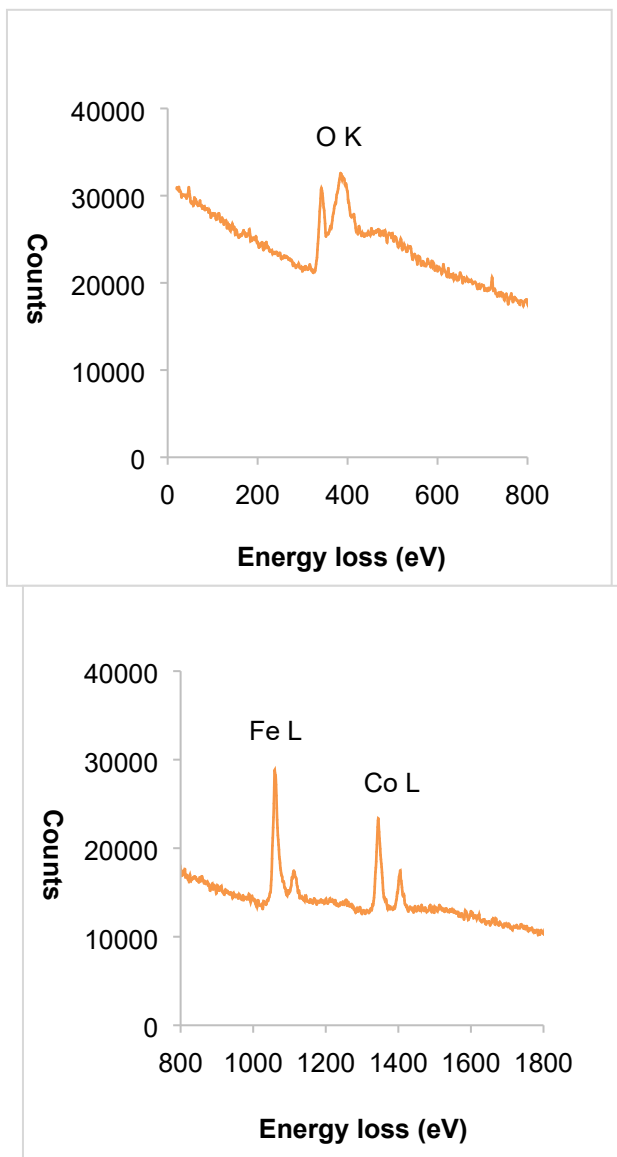


Figure S7. EELS spectra of (a) oxygen K edge of PdCo–Fe₃O₄ NPs; (b) iron and cobalt L edge of PdCo–Fe₃O₄ NPs

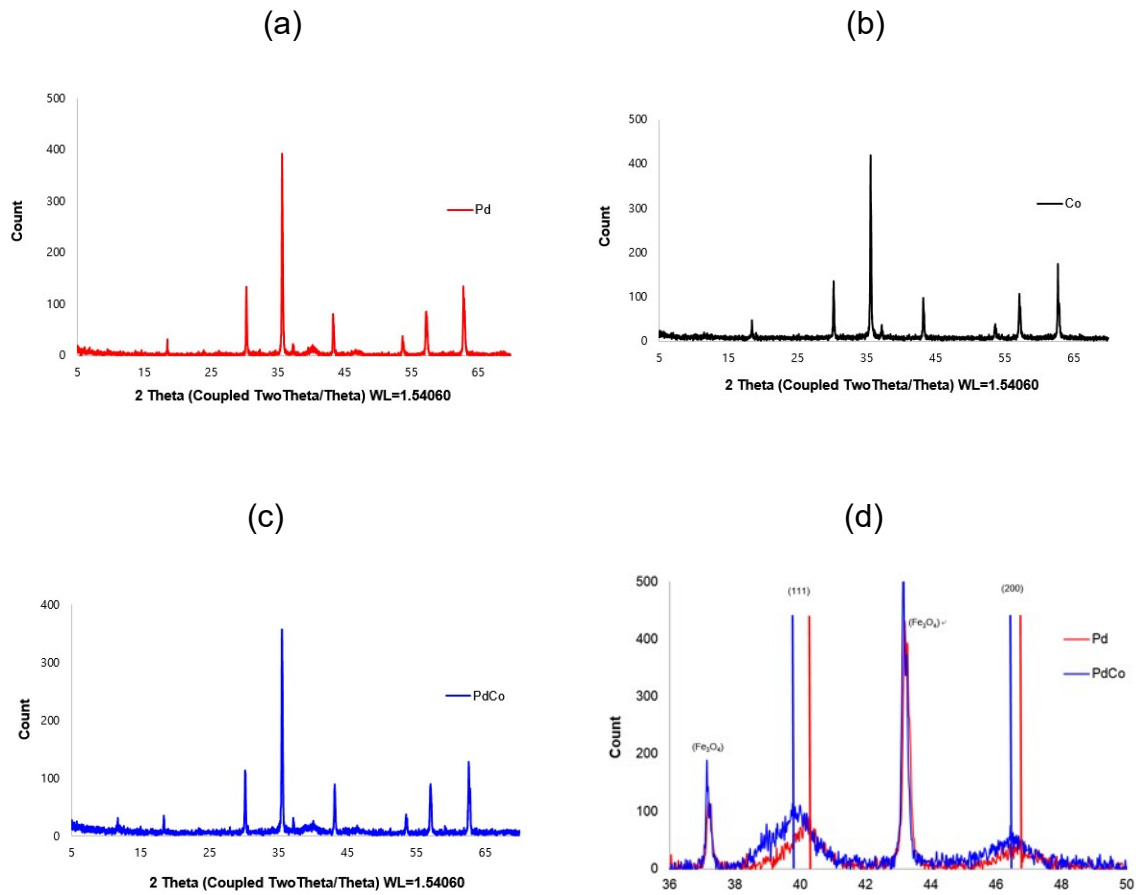
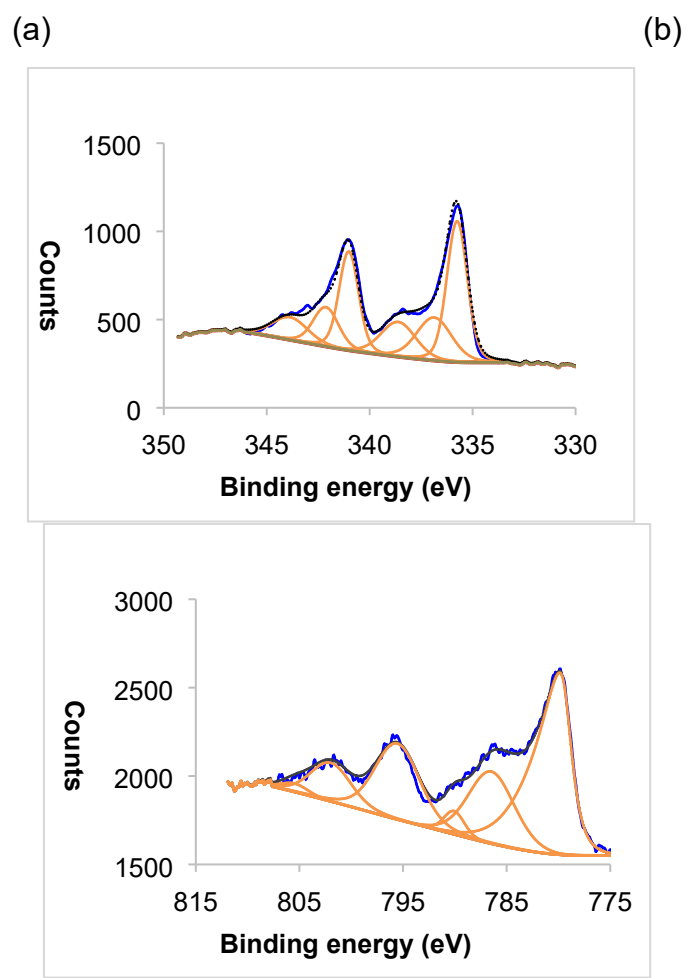


Figure S8. XRD data of (a) Pd–Fe₃O₄ NPs; (b) Co–Fe₃O₄ NPs; (c) PdCo–Fe₃O₄ NPs; and (d) Comparison of XRD peaks of the catalysts



(c) (d)

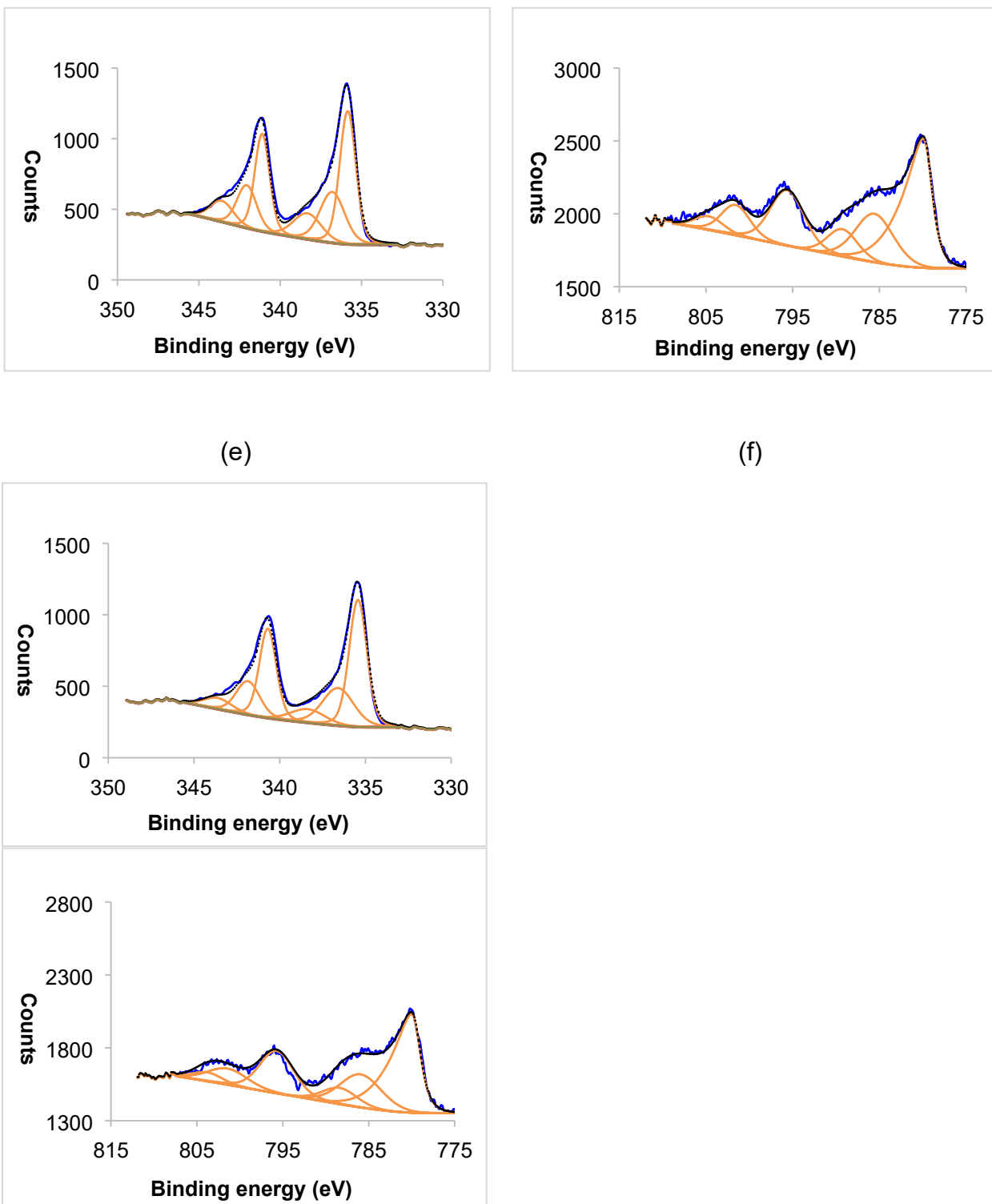
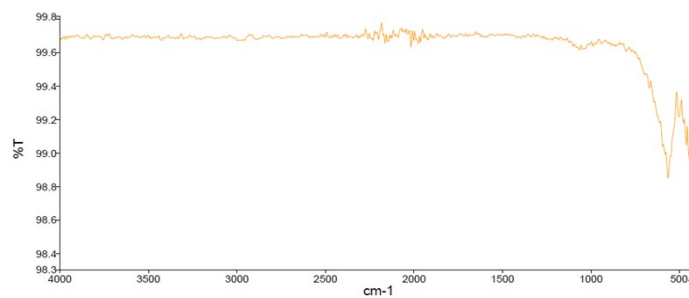


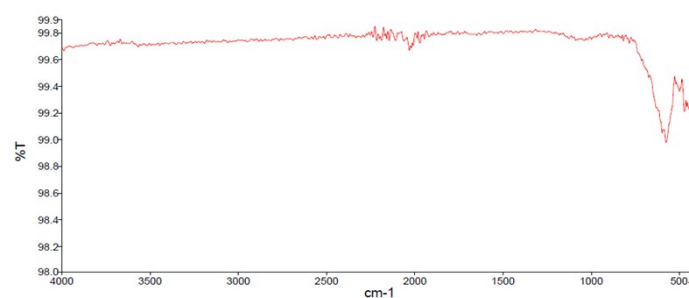
Figure S9. XPS data of (a) Pd 3d spectra of Pd–Fe₃O₄ NPs; (b) Co 2p spectra of Co–Fe₃O₄ NPs; (c) Pd 3d spectra of PdCo–Fe₃O₄ NPs; (d) Co 2p spectra of PdCo–Fe₃O₄ NPs; (e) Pd 3d spectra of PdCo–Fe₃O₄ NPs after 1 catalytic cycle; and (f) Co 2p spectra

of PdCo–Fe₃O₄ NPs after 1 catalytic cycle

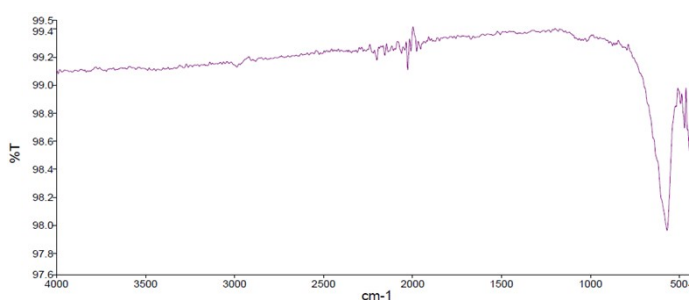
(a)



(b)



(c)



(d)

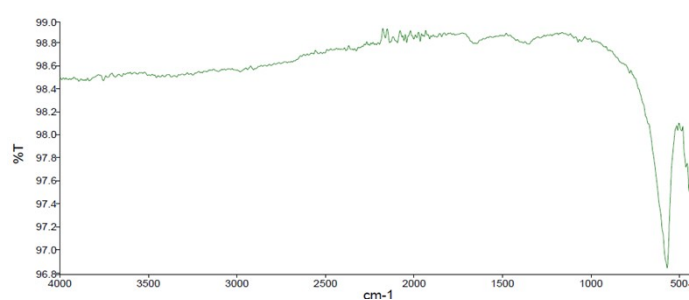


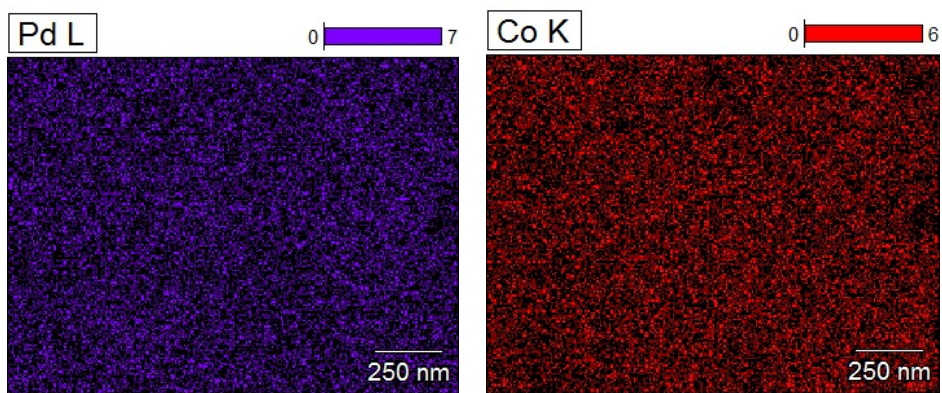
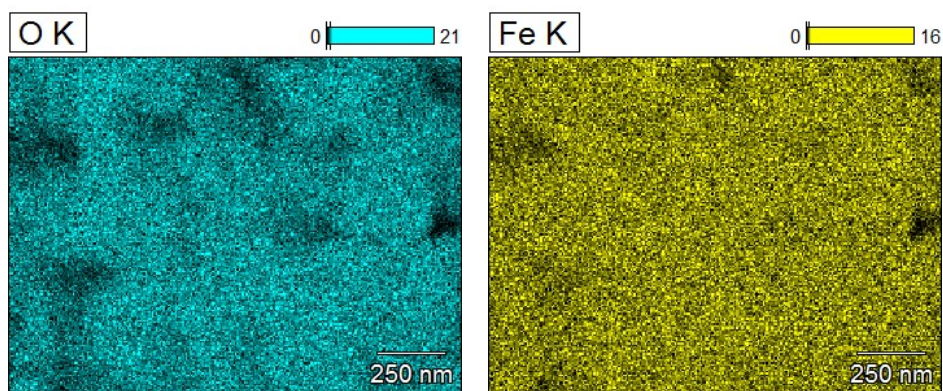
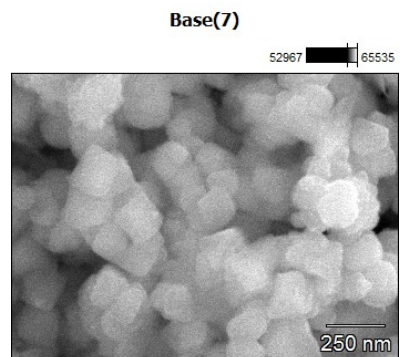
Figure S10. Fourier transform infrared (FTIR) spectra of (a) Fe₃O₄ NPs; (b) Pd–Fe₃O₄ NPs; (c) Co–Fe₃O₄ NPs; and (d) PdCo–Fe₃O₄ NPs

Catalyst	Pd (wt%)	Co (wt%)
PdCo–Fe ₃ O ₄	7.49	3.89
Pd–Fe ₃ O ₄	5.67	-
Co–Fe ₃ O ₄	-	4.31
PdCo–Fe ₃ O ₄ (after 1 st reaction)	7.34	3.23
PdCo–Fe ₃ O ₄ (after 14 th reaction)	1.69	0.28

Figure S11. ICP-AES data of PdCo–Fe₃O₄ NPs, Pd–Fe₃O₄ NPs, Co–Fe₃O₄ NPs, PdCo–Fe₃O₄ NPs after the first reaction, and PdCo–Fe₃O₄ NPs after the 14th reaction

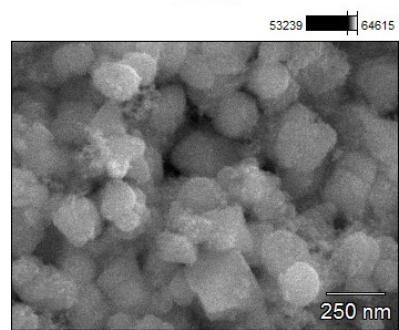
5. Supplementary data

(a)



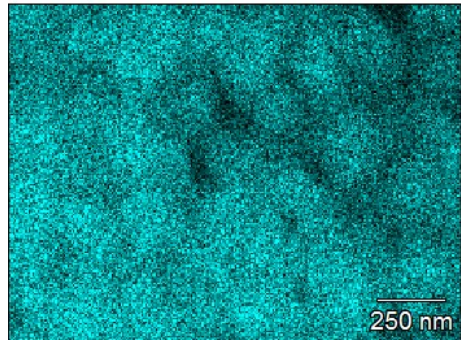
(b)

Base(9)



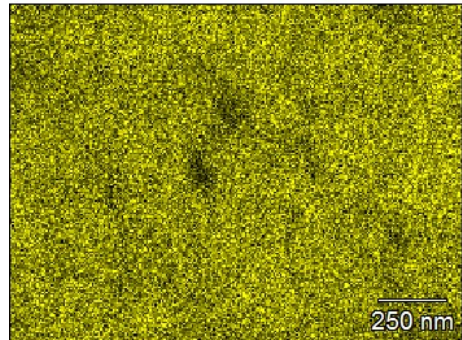
OK

0 22



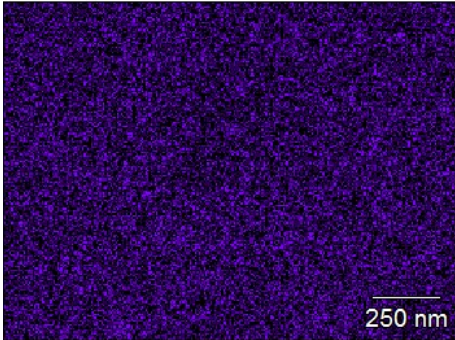
Fe K

0 18



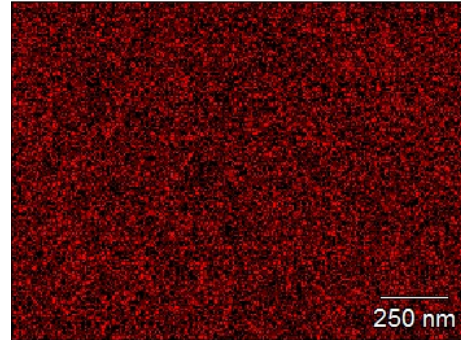
Pd L

0 8



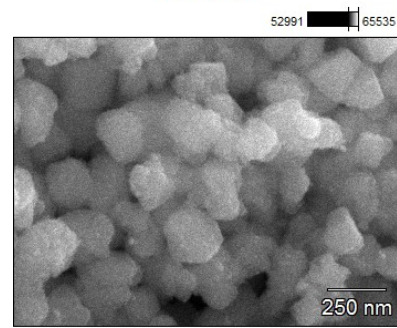
Co K

0 7



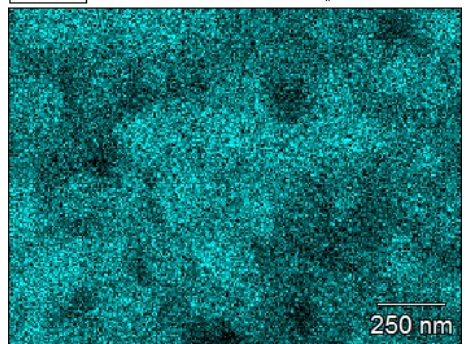
(c)

Base(11)



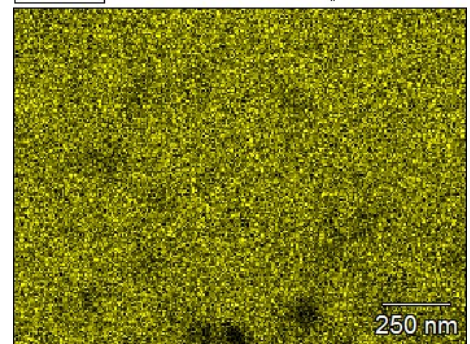
OK

0 15



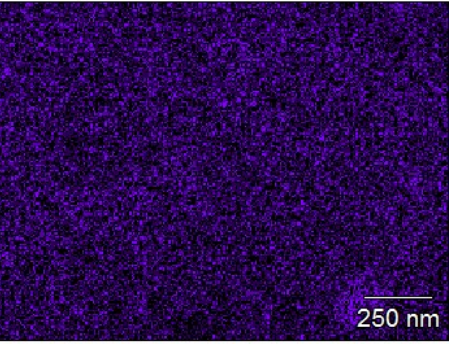
Fe K

0 14



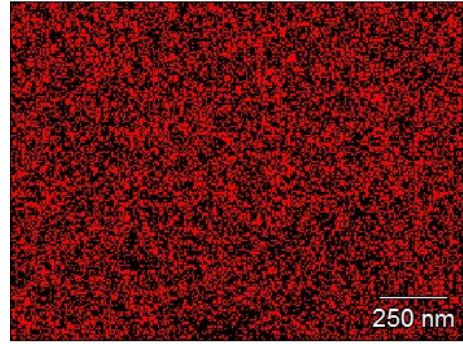
Pd L

0 7



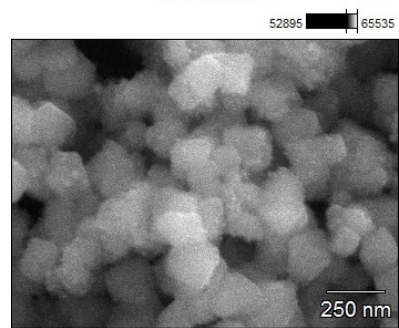
Co K

0 5



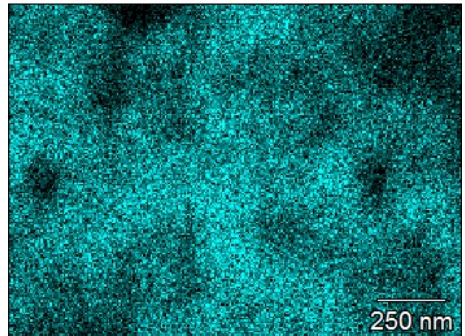
(d)

Base(13)



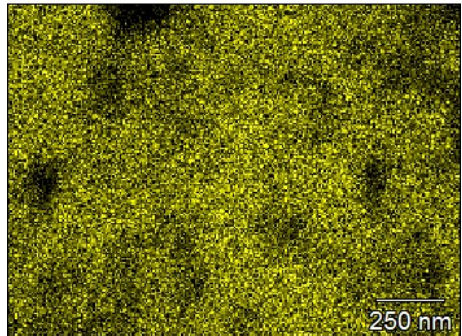
OK

0 15



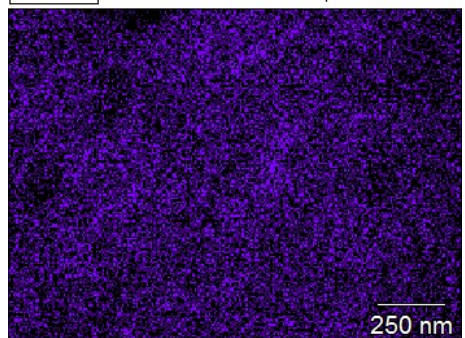
Fe K

0 12



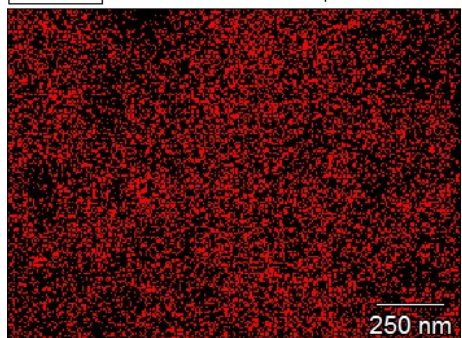
Pd L

0 7



Co K

0 6

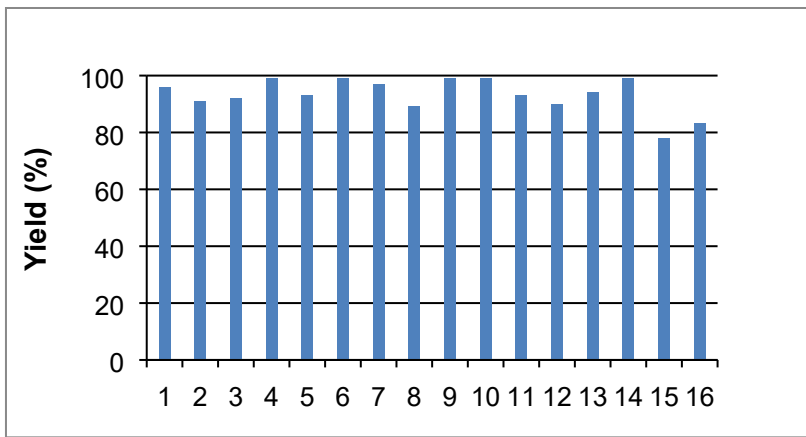


(e)

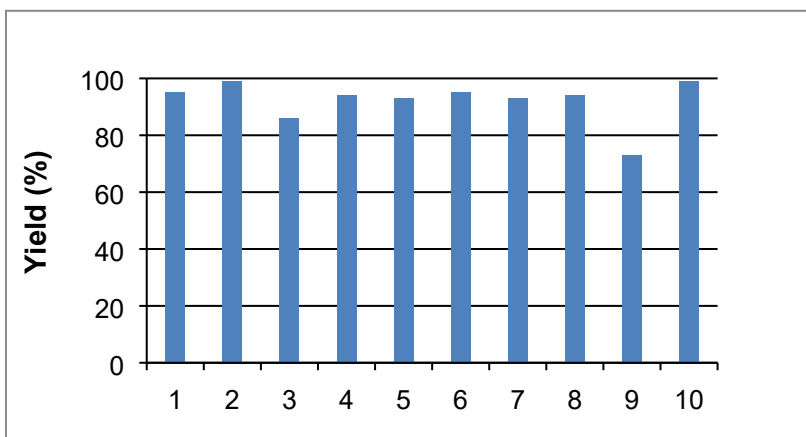
Catalyst	Pd (wt%)	Co (wt%)	Molar ratio
Pd _{0.26} Co ₁ –Fe ₃ O ₄	2.39	5.07	0.26:1
Pd _{0.46} Co ₁ –Fe ₃ O ₄	4.01	4.86	0.46:1
Pd ₁ Co ₁ –Fe ₃ O ₄	7.41	4.15	0.99:1
Pd ₁ Co _{0.45} –Fe ₃ O ₄	7.79	1.94	1:0.45
Pd ₁ Co _{0.28} –Fe ₃ O ₄	6.21	0.97	1:0.28

Figure S12. SEM and EDS images of (a) Pd_{0.26}Co₁–Fe₃O₄ NPs; (b) Pd_{0.46}Co₁–Fe₃O₄ NPs; (c) Pd₁Co_{0.45}–Fe₃O₄ NPs; (d) Pd₁Co_{0.28}–Fe₃O₄ NPs; and (e) ICP-AES data of Pd_xCo_y–Fe₃O₄ NPs

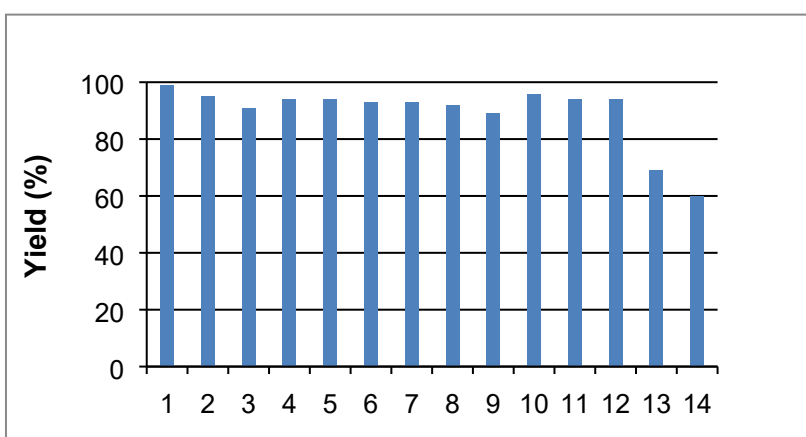
(a)



(b)



(c)



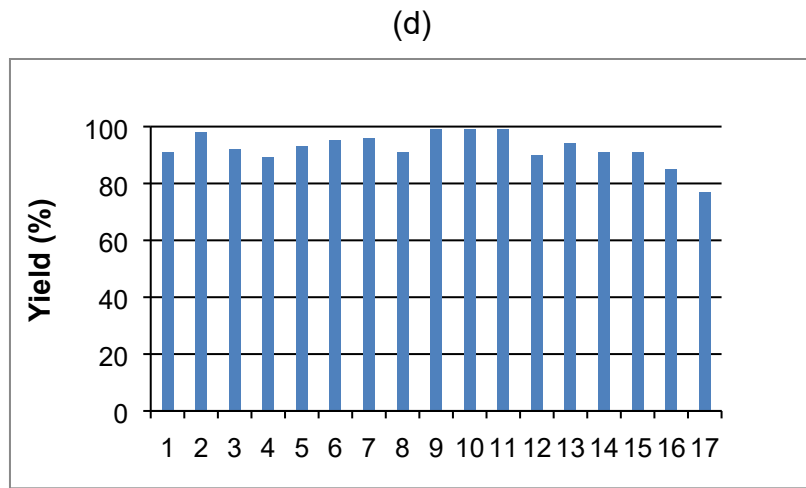


Figure S13. Recycling data of (a) $\text{Pd}_{0.26}\text{Co}_1\text{--Fe}_3\text{O}_4$ NPs; (b) $\text{Pd}_{0.46}\text{Co}_1\text{--Fe}_3\text{O}_4$ NPs; (c) $\text{Pd}_1\text{Co}_1\text{--Fe}_3\text{O}_4$ NPs, and (d) $\text{Pd}_1\text{Co}_{0.28}\text{--Fe}_3\text{O}_4$ NPs

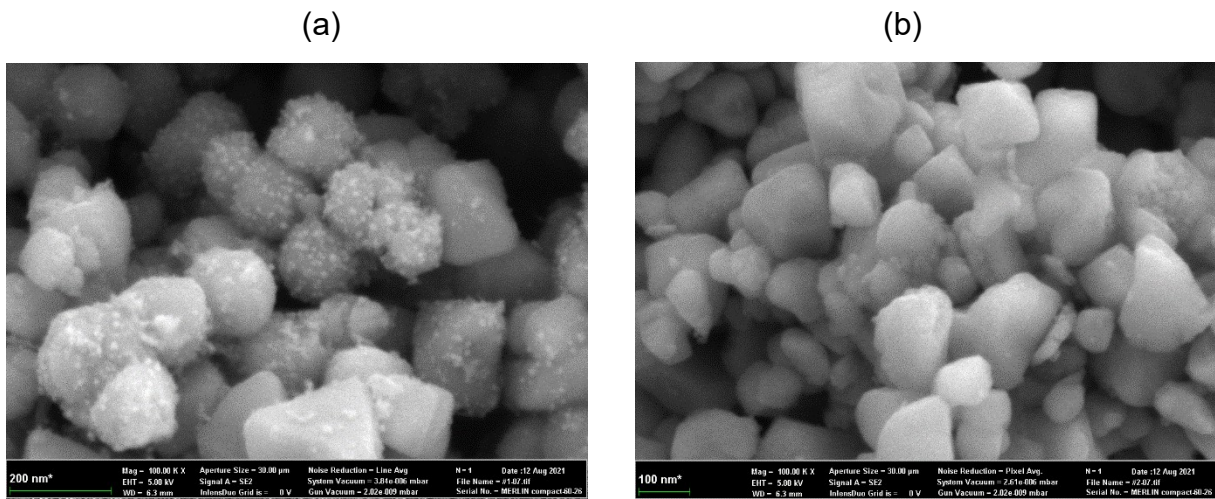


Figure S14. SEM images of $\text{PdCo}\text{--Fe}_3\text{O}_4$ NPs after 18 h under 0.20 mmol N -benzylideneaniline, 2.0 mol% $\text{PdCo}\text{--Fe}_3\text{O}_4$ after (a) 1st reaction; (b) 14th reaction

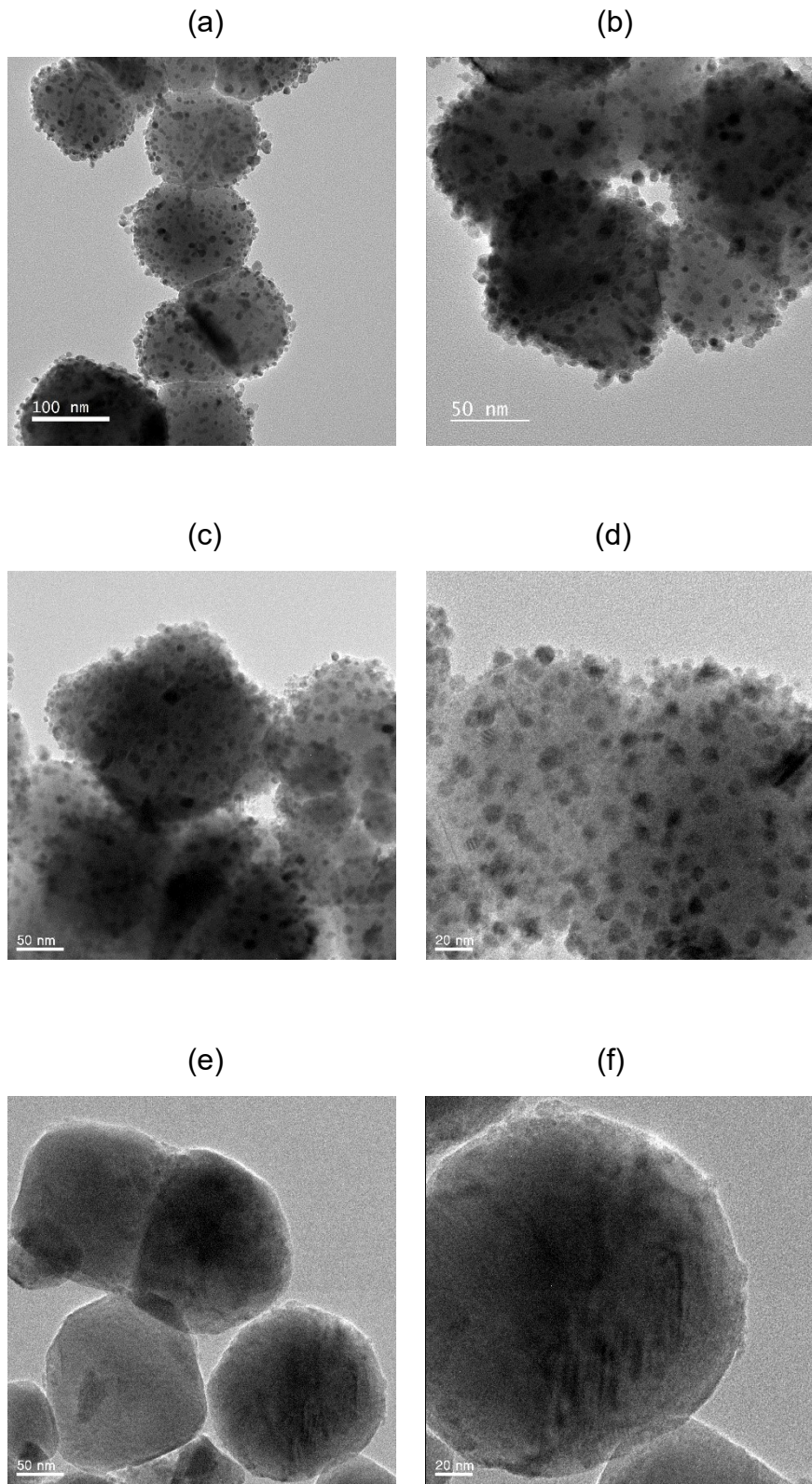


Figure S15. HR-TEM images of (a) and (b) fresh PdCo-Fe₃O₄ NPs; (c) and (d) PdCo-Fe₃O₄ NPs after 1 catalytic cycle; (e) and (f) PdCo-Fe₃O₄ NPs after 14 catalytic cycles

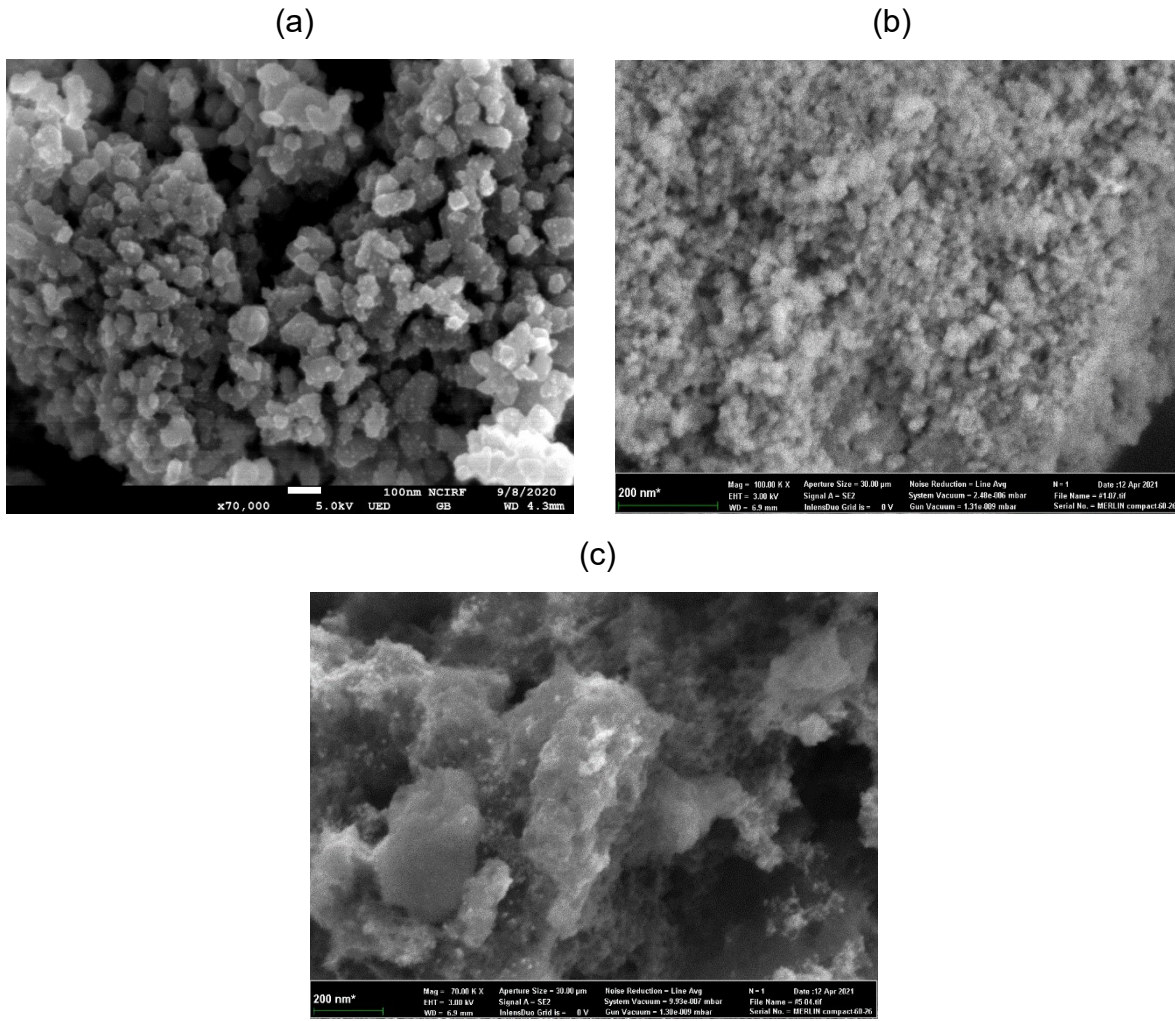


Figure S16. SEM images of (a) PdCo–TiO₂ NPs; (b) PdCo–CeO₂ NPs; and (c) PdCo–C NPs

Catalyst	Pd (wt%)	Co (wt%)	Pd:Co
PdCo–TiO ₂	5.74	3.45	0.92:1
PdCo–CeO ₂	6.27	4.86	0.71:1
PdCo–C	4.84	3.25	0.82:1

Table S5. ICP-AES data of PdCo NPs with different supports

Table S6. Yield comparison of monometallic catalysts with other substrates

Entry ^a	Catalyst	Product Yield with various R group (%) ^b				
		H	2-Me	4-OMe	4-F	2-CF ₃
1 ^c	Pd	72	75	65	49	66
2 ^d	Co	N. D. ^g	N. D. ^g	N. D. ^g	N. D. ^g	N. D. ^g
3 ^e	Pd + Co	85	68	81	65	72
4 ^f	PdCo	98	86	96	92	78

^a Reaction conditions: **1** (0.20 mmol), catalyst, H₂ (1.0 atm), DMA (1.0 mL), r. t., 18 h.

^b Determined from ¹H NMR spectral analysis through the use of anisole as an internal standard.

^c Pd–Fe₃O₄ (1.0 mol%) was used as a catalyst.

^d Co–Fe₃O₄ (1.0 mol%) was used as a catalyst.

^e Pd–Fe₃O₄ (0.50 mol%), Co–Fe₃O₄ (0.50 mol%) were used as a catalyst.

^f PdCo–Fe₃O₄ (0.50 mol%) was used as a catalyst.

^g N. D = not detected.

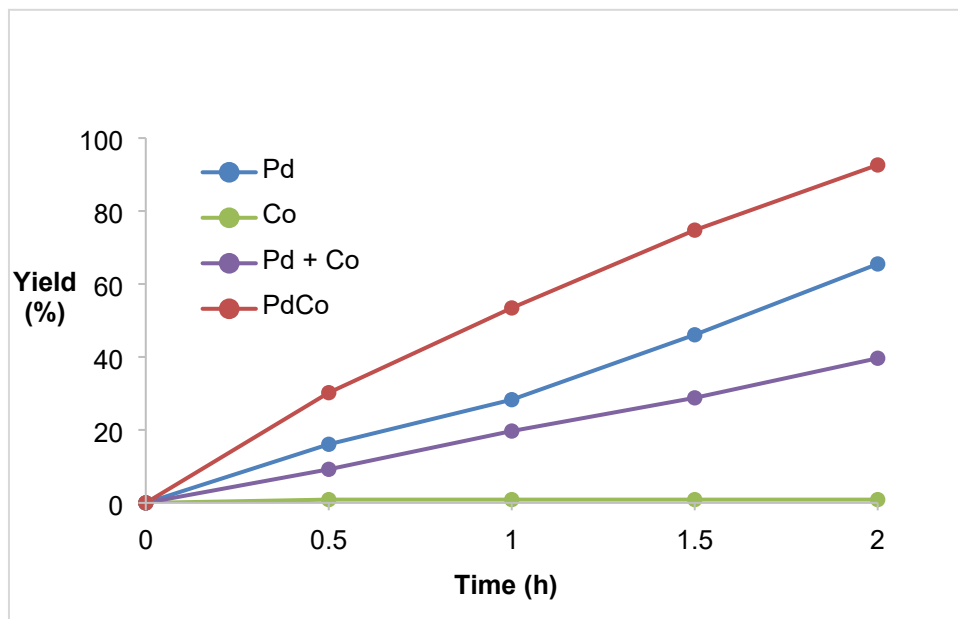
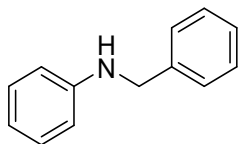


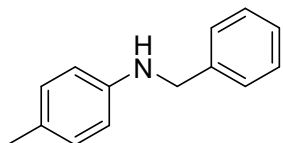
Figure S17. Initial kinetic data of *N*-benzylideneaniline (0.20 mmol scale) reduction with Pd–Fe₃O₄ NPs (1.0 mol%), Co–Fe₃O₄ NPs (1.0 mol%), a mixture of Pd–Fe₃O₄ NPs (0.05 mol%) and Co–Fe₃O₄ NPs (0.05 mol%), and PdCo–Fe₃O₄ NPs (0.50 mol%)

6. Characterization of Products



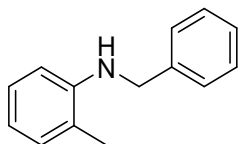
***N*-Benzylaniline (2a)**

Yellow oil. The compound was identified by spectral comparison with literature data.^[2]
¹H NMR (400 MHz, CDCl₃) δ 7.40 – 7.31 (m, 4H), 7.27 (t, J = 6.8 Hz, 1H), 7.17 (t, J = 7.9 Hz, 2H), 6.71 (t, J = 7.3 Hz, 1H), 6.63 (d, J = 7.9 Hz, 2H), 4.32 (s, 2H), 4.05 (s, 1H). ¹³C NMR (101 MHz, CDCl₃) δ 148.26, 139.55, 129.40, 128.76, 127.65, 127.36, 117.71, 112.99, 48.47.



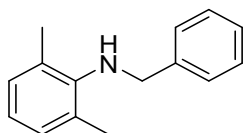
***N*-Benzyl-4-methylaniline (2b)**

Orange oil. The compound was identified by spectral comparison with literature data.^[2]
¹H NMR (400 MHz, CDCl₃) δ 7.37 – 7.31 (m, 4H), 7.26 – 7.24 (m, 1H), 6.98 (d, J = 8.1 Hz, 2H), 6.56 (d, J = 8.3 Hz, 2H), 4.30 (s, 2H), 3.91 (s, 1H), 2.23 (s, 3H). ¹³C NMR (101 MHz, CDCl₃) δ 146.05, 139.79, 129.87, 128.73, 127.62, 127.28, 126.88, 113.12, 48.78, 20.53.



***N*-Benzyl-2-methylaniline (2c)**

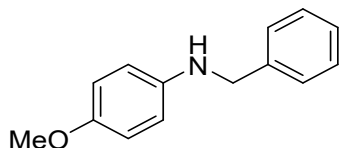
Yellow oil. The compound was identified by spectral comparison with literature data.^[2]
¹H NMR (400 MHz, CDCl₃) δ 7.38 – 7.31 (m, 4H), 7.28 – 7.25 (m, 1H), 7.10 – 7.05 (m, 2H), 6.66 (t, J = 7.3 Hz, 1H), 6.60 (d, J = 7.9 Hz, 1H), 4.35 (s, 2H), 3.83 (s, 1H), 2.14 (s, 3H). ¹³C NMR (126 MHz, CDCl₃) δ 146.18, 139.63, 130.18, 128.76, 127.35, 127.27, 122.02, 117.31, 110.12, 48.43, 17.64.



***N*-Benzyl-2,6-dimethylaniline (2d)**

Yellow oil. The compound was identified by spectral comparison with literature data.^[3]

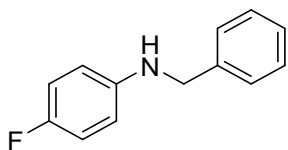
¹H NMR (400 MHz, CDCl₃) δ 7.37 – 7.27 (m, 5H), 7.00 (d, J = 7.4 Hz, 2H), 6.86 – 6.82 (m, 1H), 4.10 (s, 2H), 3.20 (s, 1H), 2.27 (s, 6H). ¹³C NMR (101 MHz, CDCl₃) δ 146.00, 140.54, 129.93, 128.95, 128.69, 128.08, 127.39, 122.30, 52.97, 18.61.



***N*-Benzyl-4-methoxyaniline (2e)**

Yellow oil. The compound was identified by spectral comparison with literature data.^[2]

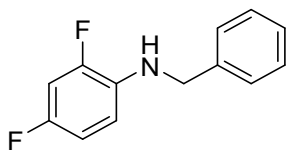
¹H NMR (400 MHz, CDCl₃) δ 7.36 – 7.25 (m, 5H), 6.76 (d, J = 8.7 Hz, 2H), 6.58 (d, J = 8.8 Hz, 2H), 4.26 (s, 2H), 3.72 (s, 3H). ¹³C NMR (101 MHz, CDCl₃) δ 152.29, 142.57, 139.81, 128.69, 127.64, 127.26, 115.02, 114.20, 55.90, 49.34.



***N*-Benzyl-4-fluoroaniline (2f)**

Yellow oil. The compound was identified by spectral comparison with literature data.^[2]

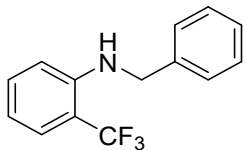
¹H NMR (400 MHz, CDCl₃) δ 7.34 – 7.37 (m, 5H), 6.86 (t, J = 8.6 Hz, 2H), 6.55 – 6.52 (m, 2H), 4.26 (s, 2H), 3.90 (s, 1H). ¹³C NMR (126 MHz, CDCl₃) δ 156.97, 155.09, 144.63, 139.39, 128.79, 127.60, 127.43, 115.87, 115.69, 113.81, 113.75, 49.07. ¹⁹F NMR (376 MHz, CDCl₃) δ -127.88 – -127.95 (m).



N-Benzyl-2,4-difluoroaniline (2g)

Yellow oil. The compound was identified by spectral comparison with literature data.^[4]

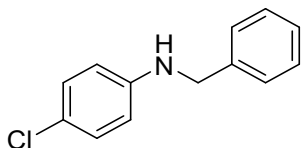
^1H NMR (400 MHz, CDCl_3) δ 7.40 – 7.27 (m, 5H), 6.82 – 6.76 (m, 1H), 6.70 (t, J = 8.6 Hz, 1H), 6.60 – 6.54 (m, 1H), 4.34 (s, 2H), 4.15 (s, 1H). ^{13}C NMR (126 MHz, CDCl_3) δ 155.42, 155.38, 153.58, 153.49, 151.97, 138.93, 128.87, 127.58, 127.50, 112.35 (dd, J = 8.8, 4.2 Hz), 110.73 (dd, J = 21.6, 3.3 Hz), 103.57 (dd, J = 26.6, 22.5 Hz), 48.46. ^{19}F NMR (376 MHz, CDCl_3) δ -125.93 – -125.99 (m), -132.15 – -132.21 (m).



N-Benzyl-2-(trifluoromethyl)aniline (2h)

Yellow oil. The compound was identified by spectral comparison with literature data.^[5]

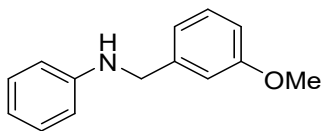
^1H NMR (400 MHz, CDCl_3) δ 7.45 (d, J = 7.8 Hz, 1H), 7.35 – 7.25 (m, 6H), 6.73 – 6.67 (m, 2H), 4.80 (s, 1H), 4.41 (d, 2H). ^{13}C NMR (101 MHz, CDCl_3) δ 145.48, 145.47, 138.55, 133.24, 128.93, 127.56, 127.24, 126.73 (q, J = 5.6 Hz), 124.01, 116.30, 113.78, 113.49, 112.30, 47.79. ^{19}F NMR (376 MHz, CDCl_3) δ -62.47.



N-Benzyl-4-chloroaniline (2i)

Yellow oil. The compound was identified by spectral comparison with literature data.^[2]

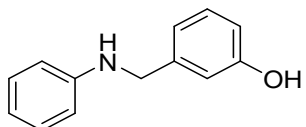
^1H NMR (400 MHz, CDCl_3) δ 7.34 (d, J = 4.3 Hz, 4H), 7.28 (dd, J = 8.7, 4.3 Hz, 1H), 7.10 (d, J = 8.8 Hz, 2H), 6.54 (d, J = 8.8 Hz, 2H), 4.30 (s, 2H), 4.08 (s, 1H). ^{13}C NMR (101 MHz, CDCl_3) δ 146.77, 139.06, 129.20, 128.84, 127.54, 127.51, 122.24, 114.04, 48.48.



N-(3-Methoxybenzyl)aniline (**2j**)

Yellow oil. The compound was identified by spectral comparison with literature data.^[6]

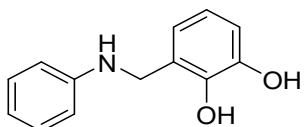
¹H NMR (400 MHz, CDCl₃) δ 7.24 (t, J = 7.8 Hz, 1H), 7.16 (t, J = 7.7 Hz, 2H), 6.97 – 6.90 (m, 2H), 6.81 (d, J = 8.1 Hz, 1H), 6.71 (t, J = 7.2 Hz, 1H), 6.62 (d, J = 7.9 Hz, 2H), 4.29 (s, 2H), 4.02 (s, 1H), 3.78 (s, 3H). ¹³C NMR (101 MHz, CDCl₃) δ 160.00, 148.24, 141.28, 129.76, 129.36, 119.83, 117.68, 113.12, 112.96, 112.74, 55.31, 48.41.



3-((Phenylamino)methyl)phenol (**2k**)

Yellow oil. The compound was identified by spectral comparison with literature data.^[4]

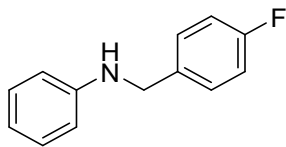
¹H NMR (400 MHz, CDCl₃) δ 7.19 – 7.14 (m, 3H), 6.89 (d, J = 7.5 Hz, 1H), 6.79 (s, 1H), 6.73 – 6.69 (m, 2H), 6.61 (d, J = 7.7 Hz, 2H), 4.24 (s, 2H). ¹³C NMR (126 MHz, CDCl₃) δ 156.05, 148.08, 141.45, 129.98, 129.41, 119.77, 117.91, 114.35 (d, J = 7.2 Hz), 113.18, 48.22.



3-((Phenylamino)methyl)benzene-1,2-diol (**2l**)

Dark red oil.

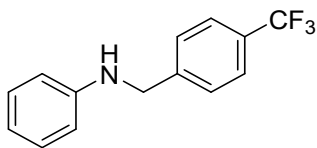
¹H NMR (400 MHz, CDCl₃) δ 7.25 (t, J = 7.6 Hz, 2H), 6.93 (t, J = 7.4 Hz, 1H), 6.89 – 6.84 (m, 3H), 6.78 (t, J = 7.8 Hz, 1H), 6.70 (d, J = 7.5 Hz, 1H), 4.41 (s, 2H). ¹³C NMR (101 MHz, CDCl₃) δ 147.16, 145.06, 143.78, 129.54, 123.07, 121.32, 120.49, 119.67, 116.29, 114.53, 48.97. HRMS (ESI) calculated for C₁₃H₁₃NO₂ [M]⁺ 215.0946, found 215.0946.



N-(4-Fluorobenzyl)aniline (**2m**)

Yellow oil. The compound was identified by spectral comparison with literature data.^[7]

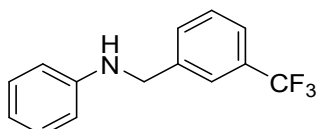
¹H NMR (400 MHz, CDCl₃) δ 7.34 – 7.40 (m, 2H), 7.17 (t, J = 7.9 Hz, 2H), 7.01 (t, J = 8.7 Hz, 2H), 6.72 (t, J = 7.3 Hz, 1H), 6.61 (d, J = 7.8 Hz, 2H), 4.29 (s, 2H), 4.01 (s, 1H). ¹³C NMR (101 MHz, CDCl₃) δ 163.38, 160.95, 148.06, 135.24, 135.21, 129.42, 129.16, 129.08, 117.86, 115.67, 115.46, 112.99, 47.74. ¹⁹F NMR (376 MHz, CDCl₃) δ -115.61 – -115.76 (m).



N-(4-(Trifluoromethyl)benzyl)aniline (**2n**)

Yellow oil. The compound was identified by spectral comparison with literature data.^[8]

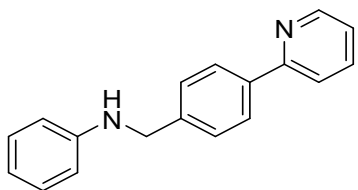
¹H NMR (400 MHz, CDCl₃) δ 7.57 (d, J = 7.9 Hz, 2H), 7.46 (d, J = 7.9 Hz, 2H), 7.16 (t, J = 7.9 Hz, 2H), 6.72 (t, J = 7.3 Hz, 1H), 6.59 (d, J = 7.7 Hz, 2H), 4.38 (s, 2H), 4.10 (s, 1H). ¹³C NMR (126 MHz, CDCl₃) δ 147.81, 143.90, 129.70, 129.47, 127.56, 125.68 (q, J = 3.6 Hz), 123.26, 118.09, 113.03, 47.91. ¹⁹F NMR (376 MHz, CDCl₃) δ -62.40.



N-(3-(Trifluoromethyl)benzyl)aniline (**2o**)

Yellow oil. The compound was identified by spectral comparison with literature data.^[9]

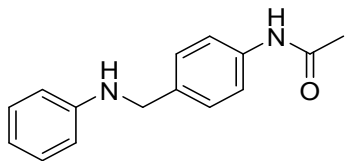
¹H NMR (400 MHz, CDCl₃) δ 7.63 (s, 1H), 7.57 – 7.52 (m, 2H), 7.44 (t, J = 7.7 Hz, 1H), 7.18 (t, J = 7.9 Hz, 2H), 6.74 (t, J = 7.3 Hz, 1H), 6.62 (d, J = 7.9 Hz, 2H), 4.39 (s, 2H), 4.10 (s, 1H). ¹³C NMR (126 MHz, CDCl₃) δ 147.87, 140.77, 131.24, 130.98, 130.77, 129.47, 129.22, 124.25, 124.23, 124.20, 124.17, 118.14, 113.07, 48.07. ¹⁹F NMR (376 MHz, CDCl₃) δ -62.58.



***N*-(4-(Pyridin-2-yl)benzyl)aniline (2p)**

Pale yellow solid. The compound was identified by spectral comparison with literature data.^[10]

¹H NMR (400 MHz, CDCl₃) δ 8.68 (d, J = 4.8 Hz, 1H), 7.97 (d, J = 8.1 Hz, 2H), 7.77 – 7.68 (m, 2H), 7.47 (d, J = 8.0 Hz, 2H), 7.25 – 7.15 (m, 3H), 6.72 (t, J = 7.3 Hz, 1H), 6.65 (d, J = 7.7 Hz, 2H), 4.39 (s, 2H), 4.11 (s, 1H). ¹³C NMR (126 MHz, CDCl₃) δ 157.32, 149.81, 148.21, 140.51, 138.57, 136.86, 129.40, 127.93, 127.31, 122.19, 120.56, 117.78, 113.07.



***N*-(4-((Phenylamino)methyl)phenyl)acetamide (2q)**

Pale yellow solid. The compound was identified by spectral comparison with literature data.^[11]

¹H NMR (400 MHz, CDCl₃) δ 7.46 (d, J = 8.2 Hz, 2H), 7.32 (d, J = 8.2 Hz, 2H), 7.22 (s, 1H), 7.17 (t, J = 7.8 Hz, 2H), 6.71 (t, J = 7.2 Hz, 1H), 6.62 (d, J = 7.9 Hz, 2H), 4.29 (s, 2H), 4.05 (s, 1H), 2.17 (s, 3H). ¹³C NMR (101 MHz, CDCl₃) δ 168.41, 148.16, 137.00, 135.55, 129.39, 128.25, 120.29, 117.73, 112.99, 47.96, 24.75.

II. References

- [1] A. K. Chakraborti, S. Bhagat, S. Rudrawar, *Tetrahedron Lett.* **2004**, *45*, 7641–7644.
- [2] L. M. Broomfield, Y. Wu, E. Martin, A. Shafir, *Adv. Synth. Catal.* **2015**, *357*, 3538–3548.
- [3] F. -D. Huang, C. Xu, D. -D. Lu, D. -S. Shen, T. Li, F. -S. Liu, *J. Org. Chem.* **2018**, *83*, 9144–9155.
- [4] W. Yang, L. Wei, F. Yi, M. Cai, *Catal. Sci. Technol.*, **2016**, *6*, 4554–4564.
- [5] K. Naksomboon, J. Poater, F. M. Bickelhaupt, M. Á. F. -Ibáñez, *J. Am. Chem. Soc.* **2019**, *141*, 6719–6725.
- [6] Y. Du, S. Oishi, S. Saito, *Chem. Eur. J.* **2011**, *17*, 12262–12267.
- [7] A. Cho, S. Byun, B. M. Kim, *Adv. Synth. Catal.* **2018**, *360*, 1253–1261.
- [8] R. Adam, J. R. C. -Antonino, K. Junge, R. Jackstell, M. Beller, *Angew. Chem. Int. Ed.* **2016**, *55*, 11049–11053.
- [9] C. Lu, Z. Qiu, M. Xuan, Y. Huang, Y. Lou, Y. Zhu, H. Shen, B. -L. Lin, *Adv. Synth. Catal.* **2020**, *362*, 4151–4158.
- [10] F. Kallmeier, R. Fertig, T. Irrgang, R. Kempe, *Angew. Chem. Int. Ed.* **2020**, *59*, 11789–11793.
- [11] S. C. A. Sousa, A. C. Fernandes, *Adv. Synth. Catal.* **2010**, *352*, 2218–2226.

III. NMR spectra

